World Scientific
www.worldscientific.com

Mechanical analogies for nonlinear light beams in nonlocal nematic liquid crystals

Gaetano Assanto

University of Rome "Roma Tre",
NooEL — Nonlinear Optics and OptoElectronics Lab,
Rome 00146, Italy

Panayotis Panayotaros

IIMAS, Universidad Nacional Autónoma de México,
Apdo. Postal 20-726, 01000 Cd. México, México

Noel F. Smyth

School of Mathematics, University of Edinburgh,
Edinburgh, Scotland, EH9 3FD, UK
N.Smyth@ed.ac.uk

The equations governing nonlinear light beam propagation in nematic liquid crystals form a $(2+1)$-dimensional system consisting of a nonlinear Schrödinger-type equation for the electric field of the wavepacket and an elliptic equation for the reorientational response of the medium. The latter is "nonlocal" in the sense that it is much wider than the size of the beam. Due to these nonlocal, nonlinear features, there are no known general solutions of the nematic equations; hence, approximate methods have been found convenient to analyze nonlinear beam propagation in such media, particularly the approximation of solitary waves as mechanical particles moving in a potential. We review the use of dynamical equations to analyze solitary wave propagation in nematic liquid crystals through a number of examples involving their trajectory control, including comparisons with experimental results from the literature. Finally, we make a few general remarks on the existence and stability of optically self-localized solutions of the nematic equations.

Keywords: Nematic liquid crystals; nematicons; solitary waves; variational approximations.

1. Introduction

Nematic liquid crystals (NLC) form an ideal medium for the manipulation and control of light. There are a number of reasons for this, including their easily controllable optical properties, for instance, refractive index, and their "huge"

reorientational nonlinearity, several orders of magnitude greater than the electronic response of optical glasses.[1,2] In particular, the large nonlinearity allows optical spatial solitary waves, termed nematicons,[3,4] to be generated at low powers by a balance between diffraction and the nonlinear (self-focusing) response of NLC.

At the most basic level, the nondimensional equations governing the propagation of an extraordinarily-polarized light beam in a birefringent (uniaxial) NLC bulk is the coupled system[3]

$$i\frac{\partial u}{\partial z} + \frac{1}{2}\nabla^2 u + 2\theta u = 0, \tag{1}$$

$$\nu\nabla^2\theta - 2q\theta = -2|u|^2. \tag{2}$$

Here, u is the (slowly varying) envelope of the electric field of the light beam and θ is the medium response to it, the extra rotation of the NLC main molecular axes from the initial orientation θ_0, with θ_0 the angle of the beam wave-vector $\boldsymbol{k}$ with respect to the optic axis $\mathbf{n}$ of the medium. The Laplacian ∇^2 is in the (x, y) plane transverse to the down-cell direction z, i.e., the propagation direction. The parameter q is proportional to the square of the external electric field applied along x to pre-orient the molecular director $\mathbf{n}$ in (x, z), i.e., when $\mathbf{n}$ is initially set at $\theta_0 = 0$ along z, as, e.g., in Refs. 3–7. Note that, $q = 0$ when there is no external electric field, as in "bias-free" configurations with $\mathbf{n}$ arranged with $\theta_0 \neq \pi/2$ and $\theta_0 \neq 0$ in the principal plane (y, z).[2,8–11] The parameter ν measures the elastic response of the NLC and is large, typically $\nu = O(100)$, in most experimental conditions.[12,13] The electric field equation (1) is a nonlinear Schrödinger (NLS) type equation and the NLC response equation (2) is a linear elliptic equation. The solution of the elliptic equation depends on u in the whole domain, implying that the medium responds "nonlocally." In principle, it could be solved through the use of a Green's function so that θ would be given by an integral of $|u|$, but as the Green's function kernel is the modified Bessel function K_0, this is not useful.

The system (1) and (2) supports optical solitary wave solutions, nematicons,[3] but there are no known general analytical solutions for it, even in $(1+1)$D, except isolated solutions for fixed parameter values.[14] While numerical methods can always be used to solve them, they tend to provide limited insight into the physics behind nematicons, their behavior and interactions. In this regard, it was realized that since solitons under interaction behave as particles,[15] hence their name, their propagation can be asymptotically modeled as mechanical particles moving in a potential well.[16] This approximation is useful for studying optical solitary waves in various nonlinear media,[17] including nematic liquid crystals.[18–21] Furthermore, it gives results in excellent agreement with experiments on nematicons in nonuniform samples.[10,11,22] In these comparisons beam propagation is modeled by the motion of a particle, whose "mass" is the beam power, in a potential induced by the change in the background director orientation (i.e., refractive index) of the nematic liquid crystal. A general review of such mechanical analogies for optical solitary waves can be found in Ref. 23.

This paper is an overview and compilation of recent work on using mechanical analogies when modeling optical solitary wave propagation in reorientational nematic liquid crystals. The equations governing beam propagation in nonlocal nonlinear NLC are introduced and set into suitable forms for a mechanical analysis. Some examples are discussed to prove their utility for analyzing experimental results, emphasizing their power and capacity for accurate predictions. It is also shown that, under the mechanical approximation, the propagation of interacting nematicons with angular momentum is governed by equations similar to those for gravitating masses, albeit with a more involved potential than Newtonian. The final two sections present theoretical considerations on existence and stability of NLC solitary waves in the presence of and due to nonlocality and saturation of the nonlinear response.

2. Optical Spatial Solitary Waves in NLC: Nematicons

The nondimensional equations (1) and (2) govern nonlinear light propagation in nematic liquid crystals in the perturbative regime (i.e., small nonlinear changes in orientation, consistent with the milliwatt powers typically employed in experiments). In the local limit $\nu \to 0$ these equations reduce to the NLS equation

$$i\frac{\partial u}{\partial z} + \frac{1}{2}\nabla^2 u + \frac{2}{q}|u|^2 u = 0. \tag{3}$$

In $(1+1)$ dimensions this equation is completely integrable via the method of inverse scattering,[15,24] so in principle its solution is known in general. In $(2+1)$ dimensions, which is the usual experimental regime, beam type initial conditions yield either catastrophic collapse in finite z if the beam power is above a critical level, or decay to diffractive radiation below this critical value.[25] However, the normal regime for nematicons is the nonlocal limit with $\nu = O(100)$,[12,13] so that the width of the medium response is much larger than the size of the optical forcing.[26–29] This nonlocal response stabilizes $(2+1)$-dimensional beams[3,4,6,7,30,31] as the NLS-type propagation equation (1) is coupled to the NLC response (2). The elliptic nature of the latter means that its solution depends on the entire domain (NLC cell), the mathematical equivalent of the physical concept of a nonlocal response. As the system (1) and (2) is coupled, to date no general solutions have been obtained for it, in particular, no nematicon solutions. In this regard, although a soliton is a particular type of solitary wave, the terms solitary wave and soliton are not strictly interchangeable, because solitons are governed by a nonlinear dispersive wave equation which is exactly integrable[15,24] and therefore, interact "cleanly" without modifications, whereas generic solitary waves can change shape on collision. The only known solitary wave solutions of (1) and (2) are isolated solutions for fixed parameter values.[14]

Let us seek nematicon solutions of the NLC equations (1) and (2) in $(1+1)$ dimensions, by setting

$$u = f(x)e^{i\sigma z}, \quad \theta = g(x), \tag{4}$$

where f is real. The system then reduces to

$$\frac{d^2f}{dx^2} + 4gf - 2\sigma f = 0, \quad \frac{d^2g}{dx^2} + \frac{2}{\nu}f^2 - \frac{2q}{\nu}g = 0. \tag{5}$$

Isolated nematicons in $(1+1)$D can be found by noting that, for $g = f/\sqrt{2\nu}$ and $\sigma = q/\nu$, these two equations become identical, with solution[14]

$$u = \frac{3q}{2\sqrt{2\nu}} \operatorname{sech}^2\left(\sqrt{\frac{q}{2\nu}}x\right)e^{iqz/\nu}, \quad \theta = \frac{3q}{4\nu}\operatorname{sech}^2\left(\sqrt{\frac{q}{2\nu}}x\right). \tag{6}$$

This exact solution is unexpected as it has the sech^2 profile of the Korteweg–de Vries (KdV) solitons,[15] rather than the sech profile of NLS solitons. Unfortunately, in the nonlocal regime with ν large, this nematicon has a small amplitude and is of limited use. In addition, it has fixed amplitude and width and is expressed in terms of the parameters of the NLC system (1) and (2). So it is not a general solitary wave solution of arbitrary amplitude, with the latter determining the width.

This derivation of an isolated, exact nematicon solution — by forcing the electric field and director equations to be the same — can be extended to $(2+1)$D by seeking nematicons of Eqs. (1) and (2) of the form

$$u = f(r)e^{i\sigma z} \quad \text{and} \quad \theta = \frac{1}{2\sqrt{2\nu}}f(r) + \frac{\sigma}{2}, \tag{7}$$

with $r^2 = x^2 + y^2$ the polar distance. We note that, in order to obtain an exact solution, the director reorientation θ does not vanish as $r \to \infty$, in contrast to $(1+1)$ dimensions. The electric field and director equations then become the ordinary differential equation

$$f_{rr} + \frac{f_r}{r} + \frac{2}{\sqrt{2\nu}}f^2 = 0. \tag{8}$$

This is the well-known Lane–Emden equation of the second kind for a cylindrically symmetric self-gravitating fluid of index two governed by Newtonian gravitation.[32] It can also be reduced to Abel's equation[33] via a change of variables. We can introduce $t = \ln r$,

$$f(r) = \frac{\phi \ln r}{r^2} \tag{9}$$

and $\phi' = \rho(\phi)$, to obtain Abel's equation for the variable ρ

$$\rho\frac{d\rho}{d\phi} - 4\rho + 4\phi + \frac{2}{\sqrt{2\nu}}\phi^2 = 0. \tag{10}$$

This classical differential equation has been recently solved,[34,35] so that, in principle, there is an (isolated) nematicon solution in $(2+1)$D. However, the exact solution of Abel's equation is highly involved and of little practical utility, as discussed in Refs. 34 and 35 with more details in Ref. 14. There is therefore a lack of solitary wave solutions on which to base the mathematical modeling of nematicons, particularly in

nonhomogeneous samples. In the absence of exact solutions, most of the study of nematicons and other nonlinear beams in NLC has been through numerical solutions,[3,4] with much of the analytical modeling based on approximations, such as variational methods.[4,23,36] One alternative to these numerical and variational methods is to treat nematicons as mechanical particles in a potential. These mechanical approximations date back to the beginnings of soliton theory[16] and have proven to be valuable, particularly for solitary waves in modulated media.[37–39] Their application in nematic liquid crystals will now be illustrated.

An alternative approach, based on ideas from Hamiltonian mechanics and leading to abstract existence results for solitary waves and information on their stability and power thresholds, will be discussed in Sec. 5. These theoretical results can complement the approximate methods and provide additional insights.

3. Nematicons in a Potential

To introduce the ideas and approximations behind treating evolving nematicons as mechanical particles in a potential well, we shall consider the simple case of a nematicon undergoing refraction/bending in a sample with a nonhomogeneous director orientation, the latter supplying the equivalent of a mechanical potential. Two limiting cases will be considered, the director orientation varying either in a direction cross-wise to the one down the cell (z) or in the down-cell direction z, respectively.

Let us examine the propagation of a linearly polarized light beam with wavenumber k in a bias-free cell containing nematic liquid crystals perfectly oriented along $\mathbf{n}$. The direction down the cell is Z, the input wavevector $\boldsymbol{k}$ is parallel to Z and the polarization of the electric field of the beam E_Y is along Y, with X completing the coordinate triad. We set ψ to be the total (linear and nonlinear) orientation angle the NLC director $\mathbf{n}$ makes with Z. In the paraxial, slowly varying envelope approximation, the electric field E_Y is governed by the nonlinear Schrödinger-type equation[3]

$$2ikn_e\frac{\partial E_Y}{\partial Z} + 2ikn_e\Delta(\psi)\frac{\partial E_Y}{\partial Y} + \nabla^2 E_Y + k^2(n_\perp^2\cos^2\psi + n_\parallel^2\sin^2\psi$$
$$- n_\perp^2\cos^2\theta_0 - n_\parallel^2\sin^2\theta_0)E_Y = 0 \tag{11}$$

with the medium response governed by the elliptic equation

$$K\nabla^2\psi + \frac{1}{4}\epsilon_0\Delta\epsilon|E_Y|^2\sin 2\psi = 0. \tag{12}$$

Here, the Laplacian ∇^2 is in the plane (X, Y) orthogonal to the propagation direction Z; the refractive indices $n_\parallel$ and $n_\perp$ are the eigenvalues for light polarized parallel and perpendicular to the optic axis $\mathbf{n}$, respectively; the optical anisotropy is $\Delta\epsilon = n_\parallel^2 - n_\perp^2 > 0$; θ_0 is the initial orientation of $\mathbf{n}$ in the plane (Y, Z) with respect to Z at rest, in the absence of the beam; the refractive index n_e determining the

phase velocity of extraordinary waves is

$$n_e^2(\psi) = \frac{n_\perp^2 n_\parallel^2}{n_\parallel^2 \cos^2\psi + n_\perp^2 \sin^2\psi}. \tag{13}$$

The coefficient Δ is related to the birefringent walk-off angle δ of extraordinary waves with the Poynting vector and wave vector in the plane (Y, Z), with $\Delta = \tan\delta$. It is given by

$$\Delta(\psi) = \frac{\Delta\epsilon \sin 2\psi}{\Delta\epsilon + 2n_\perp^2 + \Delta\epsilon \cos 2\psi}. \tag{14}$$

In the medium response equation (12), the single elastic constant approximation has been introduced, so that the elastic constants for molecular splay, bend and twist are assumed equal and given by K.[40]

The nematic equations (11) and (12) are highly nonlinear and coupled, so they are difficult to analyze analytically. However, in most experiments in purely dielectric NLC (without dopants), milliwatt power beams are typically employed and thermal effects can be neglected[3,4] (for the interplay between thermal and reorientational effects in dye-doped NLC see Refs. 9, 41–43). In this limit, the optically induced reorientation θ is small compared with the rest angle θ_0. To allow for a variation of the background orientation θ_0 in y and z, we set $\theta_0 = \bar\theta_0 + \theta_b$, where $\bar\theta_0$ denotes the mean of the background distribution. We further assume that the total variation of the background angle and its rate of change are small, $|\theta|, |\theta_b| \ll \bar\theta_0$. The total director angle in the presence of the light beam is then $\psi = \bar\theta_0 + \theta_b + \theta$, and the nematic equations (11) and (12) can be simplified using Taylor series for the trigonometric functions. As well as linearizing the trigonometric functions, the equations can be nondimensionalized in the space variables X, Y and Z and electric field u with

$$X = Wx, \quad Y = Wy, \quad Z = Bz, \quad E_Y = Au. \tag{15}$$

Suitable scalings are

$$W = \frac{\lambda}{\pi\sqrt{\Delta\epsilon \sin 2\bar\theta_0}}, \quad B = \frac{2n_e\lambda}{\pi\Delta\epsilon \sin 2\bar\theta_0}, \quad A^2 = \frac{2P_0}{\pi\Gamma W_b^2}, \quad \Gamma = \frac{1}{2}\epsilon_0 c n_e \tag{16}$$

for a Gaussian input beam of power P_0, width W_b and wavelength $\lambda = 2\pi/k$.[12] With these dimensionless variables, the nematic equations (11) and (12) become

$$i\frac{\partial u}{\partial z} + i\gamma_\Delta \Delta(\bar\theta_0 + \theta_b)\frac{\partial u}{\partial y} + \frac{1}{2}\nabla^2 u + 2(\theta_b + \theta)u = 0, \tag{17}$$

$$\nu\nabla^2\theta = -2|u|^2, \tag{18}$$

and the nondimensional elasticity ν and the walk-off factor γ_Δ are given by

$$\gamma_\Delta = \frac{2n_e}{\sqrt{\Delta\epsilon \sin 2\bar\theta_0}} \quad \text{and} \quad \nu = \frac{8K}{\epsilon_0 \Delta\epsilon A^2 W^2 \sin 2\bar\theta_0}. \tag{19}$$

While the low-power assumption simplifies the model, the low-power nematic equations (17) and (18) are still nonlinear, coupled and $(2+1)$-dimensional. For these reasons they have no known analytical solitary wave solutions, with the exception of isolated solutions for fixed parameter values in a homogeneous medium (that is with $\theta_b = 0$).[14] However, a detailed knowledge of a nematicon profile is not needed if only its trajectory is required,[10,11,19,22,44] because the medium is highly nonlocal,[3] with $\nu = O(100)$.[10,12,13,22] The NLC then forms a wide potential well which largely traps any radiation shed by a nematicon as it evolves, so that it reaches a steady state on a very long z scale. Since a typical NLC cell is of length $\sim 1\,\mathrm{mm}$, the trajectory of a nematicon in an experiment is little affected by shed diffractive radiation. This deduction will be verified in detail below, when mechanical equations for nematicon trajectories in a nonuniform sample are obtained.

Let us now derive mechanical equations for the trajectory of a nematicon propagating through a sample with nonuniform background orientation. The simplest approach is a Lagrangian formulation of Eqs. (17) and (18), noting that Nöther's theorem relates conservation equations to a Lagrangian formulation. The system (17) and (18) has the Lagrangian

$$L = i(u^*u_z - uu_z^*) + i\gamma_\Delta\Delta(\bar{\theta}_0 + \theta_b)(u^*u_y - uu_y^*) - |\nabla u|^2 + 4(\theta_b + \theta)|u|^2 - \nu|\nabla\theta|^2,$$
(20)

where the * superscript denotes the complex conjugate and subscripts denote derivatives. We make no assumptions on the beam profile and the NLC response, and take the general forms for the electric field u and the all-optical reorientation θ to be

$$u = af_e(\rho)e^{i\sigma+iV(y-\xi)} \quad \text{and} \quad \theta = \alpha f_d(\mu),$$
(21)

where

$$\rho = \frac{\sqrt{x^2 + (y-\xi)^2}}{w}, \quad \mu = \frac{\sqrt{x^2 + (y-\xi)^2}}{\beta}.$$
(22)

Here, f_e and f_d are the unknown profiles of the electric field and director distribution, respectively. In these solutions, V and ξ play the role of the velocity and position of the nematicon as a mechanical equivalent. Substituting the profiles (21) into the Lagrangian (22) and averaging by integrating in x and y from $-\infty$ to ∞ gives the averaged Lagrangian[15]

$$\mathcal{L} = -2S_2(\sigma' - V\xi')a^2w^2 - S_{22}a^2 - S_2(V^2 + 2VF_1 - 4F)a^2w^2 + \alpha a^2w^2 S_m - 4\nu S_{42}\alpha^2,$$
(23)

where primes denote differentiation with respect to z. Here, F and F_1, determining the beam trajectory, are expressed by

$$F(\xi) = \frac{\displaystyle\int_{-\infty}^{\infty}\!\!\int_{-\infty}^{\infty}\theta_b f_e^2\,dxdy}{\displaystyle\int_{-\infty}^{\infty}\!\!\int_{-\infty}^{\infty}f_e^2\,dxdy},$$
(24)

$$F_1(\xi) = \frac{\int_{-\infty}^{\infty}\int_{-\infty}^{\infty} \gamma_\Delta \Delta(\bar{\theta}_0 + \theta_b) f_e^2 \, dx \, dy}{\int_{-\infty}^{\infty}\int_{-\infty}^{\infty} f_e^2 \, dx \, dy}. \tag{25}$$

Finally, the integrals S_2, S_m, S_{22} and S_{42} appearing in Eq. (23) are

$$S_2 = \int_0^\infty \zeta f_e^2(\zeta) d\zeta, \quad S_{22} = \int_0^\infty \zeta f_e'^2(\zeta) d\zeta, \quad S_m = \int_0^\infty f_d(w\zeta/\beta) f_e^2(\zeta) d\zeta,$$

$$S_{42} = \frac{1}{4} \int_0^\infty \zeta \left[\frac{d}{d\zeta} f_d(\zeta) \right]^2 d\zeta. \tag{26}$$

Despite the fact that these integrals cannot be explicitly determined without knowing the profiles f_e and f_d, it will be found that their values are not needed.

The mechanical equations for the nematicon in the nonuniform medium are found as variational equations of the averaged Lagrangian (23). As we are only interested in the trajectory, we take variations with respect to ξ and V and obtain the modulation equations

$$\frac{d}{dz} a^2 w^2 V = \left[2\frac{dF}{d\xi} - V\frac{dF_1}{d\xi} \right] a^2 w^2, \tag{27}$$

$$\frac{d\xi}{dz} = V + F_1, \tag{28}$$

which determine the trajectory. Equation (27) is Newton's second law for the beam, equivalent to the equation for a mechanical particle with mass $a^2 w^2$ and velocity V acted on by a force $\mathcal{F} = (2F - VF_1)a^2 w^2$. However, unlike Newtonian mechanics, the force depends explicitly on the "mass" and velocity of the particle (beam),[18,20,45] and is significant when the interaction of nematicons is considered, see Sec. 4. Since the momentum equation (27) contains the beam power $a^2 w^2$, in principle we need to know the beam profile. However, due to the large nonlocality ν, the beam sheds little radiation as it evolves and its power is conserved to an excellent approximation. Hence, (27) becomes

$$\frac{dV}{dz} = 2\frac{dF}{d\xi} - V\frac{dF_1}{d\xi}. \tag{29}$$

The integrals F and F_1 in Eq. (29) still contain the unknown electric field profile f_e. However, $\bar{\theta}_0$ is a constant and, in addition, θ_b is slowly varying relative to the width of the beam, typically $\theta_b' \sim 0.002\,\text{rad}/\mu\text{m}$[10,22]; so, a typical length scale for the variation of the background orientation is $500\,\mu\text{m}$, while the typical beam size is a few μm. With these slowly varying assumptions, the trajectory integrals F and F_1 can be approximated by

$$F(\xi) \sim \theta_b(\xi),$$

$$F_1(\xi) \sim \gamma_\Delta \Delta(\bar{\theta}_0 + \theta_b(\xi)) = \gamma_\Delta \Delta(\bar{\theta}_0) + \gamma_\Delta \Delta'(\bar{\theta}_0)\theta_b(\xi) + \cdots \tag{30}$$

The trajectory equations (28) and (29) then reduce to the simple form

$$\frac{dV}{dz} = (2 - V\gamma_\Delta \Delta'(\bar{\theta}_0))\theta'_b(\xi), \tag{31}$$

$$\frac{d\xi}{dz} = V + \gamma_\Delta \Delta(\bar{\theta}_0) + \gamma_\Delta \Delta'(\bar{\theta}_0)\theta_b(\xi). \tag{32}$$

Let us now compare solutions of the mechanical equations (31) and (32) with recent experimental results.[10] In these measurements, a linear variation in the background director orientation was imposed across the NLC sample in the y direction. We take the angles at the two ends of the sample to be θ_i at $y = 0$ and θ_L at $y = L$ for a cell of (dimensionless) width L, so that

$$\bar{\theta} = \frac{1}{2}(\theta_i + \theta_L), \quad \theta_b(y) = \frac{\theta_L - \theta_i}{L}y + \frac{1}{2}(\theta_i - \theta_L). \tag{33}$$

For such a linear variation, the momentum equations (28) and (29) have the exact solution

$$\xi = \left[\xi_0 + \frac{1 + \gamma_\Delta^2 \Delta'(\bar{\theta}_0)\Delta(\bar{\theta}_0)}{\gamma_\Delta^2 \Delta'^2(\bar{\theta}_0)\theta'_b}\right] e^{\gamma_\Delta \Delta'(\bar{\theta}_0)\theta'_b z} - \frac{2 + \gamma_\Delta^2 \Delta'(\bar{\theta}_0)\Delta(\bar{\theta}_0)}{\gamma_\Delta^2 \Delta'^2(\bar{\theta}_0)\theta'_b}$$
$$+ \frac{1}{\gamma_\Delta^2 \Delta'^2(\bar{\theta}_0)\theta'_b} e^{-\gamma_\Delta \Delta'(\bar{\theta}_0)\theta'_b z} \tag{34}$$

as θ'_b is a constant, where ξ_0 is the input position of the beam.

Representative comparisons between the predictions of the mechanical equations (31) and (32) (with solution (34)) and experimental results from[10] are shown in Fig. 1. Clearly, the mechanical equations yield trajectories in near perfect agreement with the measured ones. References 10 and 22 provide more extensive comparisons
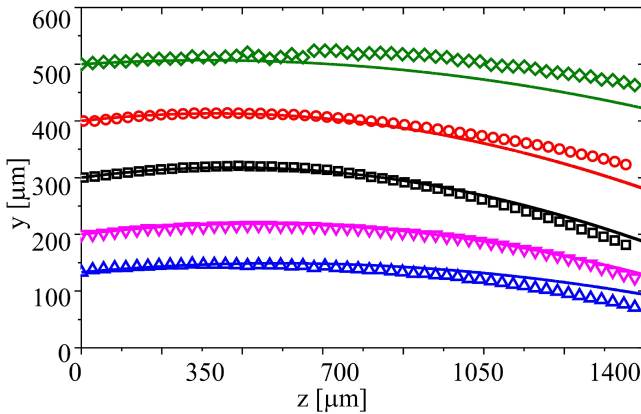

Fig. 1. Nematicon trajectories in an NLC sample nonuniform in the transverse Y direction. The background angle varies linearly from $\theta_0 = 90°$ at $Y = 0\,\mu$m to $\theta_0 = 0°$ at $Y = 600\,\mu$m. Experimental data: symbols; dynamical equations: lines. The input beam is a $2\,$mW Gaussian beam of waist $3\,\mu$m and wavelength $1.064\,\mu$m. Results from Ref. 10.

between solutions of (31) and (32), experimental data and numerical solutions of the full nematic equations, with excellent matches in all cases. These comparisons illustrate the power of the mechanical analogy for nematicon evolution. The mechanical equations (31) and (32), which are forms of Newton's second law, are a gross simplification of the full nematic set (11) and (12). At variance with numerical solutions of the full nematic equations, which require significant computational power,[22] the mechanical equations (31) and (32) model, in a highly condensed form, the interaction/evolution of the beam with/in the varying background orientation, a type of insight hardly obtainable from numerical data.

The power of mechanical analogies will be further illustrated by extending the analysis above to nematicon bending in the presence of a background orientation modulated along Z.[11]

The sample and beam set-up are as in the previous example of Y-dependent director orientation. We now take the director angle at the beginning of the cell to be $\theta_0(0)$ and the extra Z-dependent orientation change down the sample length to be $\theta_b(Z)$. We assume again that the all-optical reorientation θ is much smaller than the imposed background. The nematic equations (11) and (12) become

$$
2ikn_e \frac{\partial E_Y}{\partial Z} + 2ikn_e \Delta(\theta_0(0) + \theta_b)\frac{\partial E_Y}{\partial Y} + \nabla^2 E_Y + k^2 n_\perp^2 [\cos^2(\theta_0(0) + \theta_b)
$$
$$
- \cos^2\theta_0(0)]E_Y + k^2 n_\parallel^2 [\sin^2(\theta_0(0) + \theta_b) - \sin^2\theta_0(0)]E_Y
$$
$$
+ k^2 \Delta\epsilon \sin 2(\theta_0(0) + \theta_b)\theta E_Y = 0, \tag{35}
$$

$$
K\nabla^2\theta + \frac{1}{4}\epsilon_0 \Delta\epsilon|E_Y|^2 \sin 2(\theta_0(0) + \theta_b) = 0 \tag{36}
$$

on expanding the trigonometric functions in Taylor series for $|\theta| \ll |\theta_0(0) + \theta_b|$. As the angular variation only depends on the time-like variable Z, the electric field equation (35) can be further simplified using the phase transformation

$$
E_Y = \tilde{E}_Y \times \exp\left(\frac{ik}{2n_e}\int_0^Z [n_\perp^2(\cos^2(\theta_0(0) + \theta_b(Z)) - \cos^2\theta_0(0))\right.
$$
$$
\left. + n_\parallel^2(\sin^2(\theta_0(0) + \theta_b(Z)) - \sin^2\theta_0(0))]dZ\right). \tag{37}
$$

After this, the dimensional nematic equations become

$$
2ikn_e \frac{\partial \tilde{E}_Y}{\partial Z} + 2ikn_e \Delta(\theta_0(0) + \theta_b)\frac{\partial \tilde{E}_Y}{\partial Y} + \nabla^2 \tilde{E}_Y + k^2 \Delta\epsilon \sin 2(\theta_0(0) + \theta_b)\theta \tilde{E}_Y = 0,
$$
$$
\tag{38}
$$

$$
K\nabla^2\theta + \frac{1}{4}\epsilon_0 \Delta\epsilon|\tilde{E}_Y|^2 \sin 2(\theta_0(0) + \theta_b(Z)) = 0. \tag{39}
$$

As for the Y-dependent variation, it is easiest for subsequent analysis that the nematic equations are set in nondimensional form using the scalings W for the

transverse directions, D for the longitudinal direction and E for the electric field:

$$X = Wx, \quad Y = Wy, \quad Z = Dz, \quad \tilde{E}_Y = Eu. \tag{40}$$

Suitable scalings are, as before,

$$W = \frac{\lambda}{\pi\sqrt{\Delta\epsilon\sin 2\theta_0(0)}}, \quad D = \frac{2n_e\lambda}{\pi\Delta\epsilon\sin 2\theta_0(0)}, \quad E^2 = \frac{2P_0}{\pi\Gamma W_b^2}. \tag{41}$$

Hence, the final nondimensional form of the nematic equations with the imposed Z-modulated orientation is

$$i\frac{\partial u}{\partial z} + i\gamma_\Delta\Delta(\theta_0(0) + \theta_b(z))\frac{\partial u}{\partial y} + \frac{1}{2}\nabla^2 u + 2\frac{\sin 2(\theta_0(0) + \theta_b(z))}{\sin 2\theta_0(0)}\theta u = 0, \tag{42}$$

$$\nu\nabla^2\theta + 2\frac{\sin 2(\theta_0(0) + \theta_b(z))}{\sin 2\theta_0(0)}|u|^2 = 0, \tag{43}$$

with the Laplacian ∇^2 in the transverse variables (x, y). The walkoff parameter γ_Δ and the dimensionless elasticity ν are

$$\gamma_\Delta = \frac{2n_e}{\sqrt{\Delta\epsilon\sin 2\theta_0(0)}} \quad \text{and} \quad \nu = \frac{8K}{\epsilon_0\Delta\epsilon E^2 W^2\sin 2\theta_0(0)}. \tag{44}$$

There is no need to additionally assume that the extra imposed variation $\theta_b(z)$ is small, as was done for the y-dependent case, because the mechanical equations derived below can be solved regardless.

Similar to the Y variation, mechanical equations for the trajectory can be derived from the Lagrangian formulation of Eqs. (42) and (43). The pertinent Lagrangian is

$$L = i(u^*u_z - uu_z^*) + i\gamma_\Delta\Delta(\theta_0(0) + \theta_b(z))(u^*u_y - uu_y^*)$$
$$- |\nabla u|^2 + 4\frac{\sin 2(\theta_0(0) + \theta_b(z))}{\sin 2\theta_0(0)}\theta|u|^2 - \nu|\nabla\theta|^2. \tag{45}$$

To obtain the mechanical equations for the beam, this Lagrangian is averaged using the forms (21) with no assumptions on the actual beam and director distribution profiles. The averaged Lagrangian is found as

$$\mathcal{L} = -2S_2(\sigma' - V\xi')a^2w^2 - S_{22}a^2 - S_2[V^2 + 2V\gamma_\Delta\Delta(\theta_0(0) + \theta_b(z))]a^2w^2$$
$$+ 4\frac{\sin 2(\theta_0(0) + \theta_b(z))}{\sin 2\theta_0(0)}\alpha a^2 w^2 S_m - 4\nu S_{42}\alpha^2, \tag{46}$$

where the integrals S_i and $S_{i,j}$ are given by (26). Taking variations of the averaged Lagrangian (46) with respect to V and ξ we obtain the mechanical equations, equivalent to Newton's second law, as

$$\frac{dV}{dz} = 0, \tag{47}$$

G. Assanto, P. Panayotaros & N. F. Smyth

$$\frac{d\xi}{dz} = V + \gamma_\Delta \Delta(\theta_0(0) + \theta_b(z)), \tag{48}$$

which determine the beam trajectory. Since z is a time-like variable, there is no change in the velocity of the beam (no refraction). As for the previous example, we assumed that the beam power is constant, so that $a^2 w^2$ can be factored out of the primitive form of Eq. (47), $d/dz(a^2 w^2 V) = 0$.

Considering the experimental report in Ref. 11 with a linear variation $\theta_b(z)$ on $[0, L_n]$ and $\theta_b(L_n) = \theta_r$, we have

$$\theta_b(z) = mz, \quad m = \frac{\theta_r - \theta_0(0)}{L_n}. \tag{49}$$

With this background modulation, the position equation (48) has the solution

$$\xi = \xi_0 + Vz - \frac{\gamma_\Delta}{2m} \ln \frac{\Delta\epsilon + 2n_\perp^2 + \Delta\epsilon \cos 2(\theta_0(0) + mz)}{\Delta\epsilon + 2n_\perp^2 + \Delta\epsilon \cos 2\theta_0(0)}. \tag{50}$$

Figure 2 shows comparisons, similar to Fig. 1, of the measured nematicon trajectories of Ref. 11 and the predictions of the mechanical equations (47) and (48): the agreement is excellent, as above. The experimental results show that the nematicon trajectory is nearly independent of the beam power, as predicted by the mechanical equations. This observation validates the assumed conservation of beam power down the cell, which allowed us to neglect the variation of $a^2 w^2$, leading to the velocity equation (47).
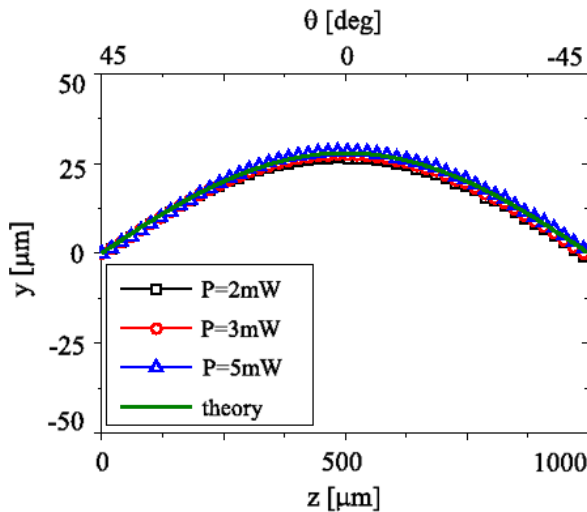

Fig. 2. (Color online) Nematicon trajectories in an NLC sample with orientation modulated in the propagation direction Z. The background angle varies linearly from $\theta_0 = 45°$ at $Z = 0 \, \mu m$ to $\theta_0 = -45°$ at $Z = 1000 \, \mu m$. Experimental data: symbols; dynamical equations: green line. The input beam is of waist $3 \, \mu m$ and wavelength $1.064 \, \mu m$, with the powers as indicated. Results from Ref. 11.

4. Kepler Nematicons

The previous examples on modeling nematicon propagation in nonuniform NLC using simple mechanical analogies can be extended to more complicated cases, such as those involving the interaction of nematicons. We consider NLC homogeneously oriented at θ_0 relative to the down-cell direction z and, for mathematical simplicity, also assume that this background orientation is due to a voltage applied across the cell, with the low-frequency electric field across x as the polarization of the input beams. We model the incoherent interaction of two extraordinarily co-polarized beams (of possibly different wavelengths) launched into the cell along z and self-confined through reorientation in the principal plane (x, z). The nondimensional equations governing the propagation and interaction of these two beams are then[46]

$$i\frac{\partial u}{\partial z} + \frac{1}{2}\nabla^2 u + 2u\theta = 0, \tag{51}$$

$$i\frac{\partial v}{\partial z} + \frac{1}{2}\nabla^2 v + 2v\theta = 0, \tag{52}$$

$$\nu\nabla^2\theta - 2q\theta = -2|u|^2 - 2|v|^2. \tag{53}$$

Here, u and v are the complex valued envelopes of the electric fields of the beams and θ is the optically induced reorientation above the background θ_0, with q proportional to the square of the electric field of the voltage imposing θ_0. If the beams have distinct colors, the coefficients of the Laplacians $\nabla^2 u$ and $\nabla^2 v$ are different. However, for the experimental case of near-infrared and visible beams as in Ref. 46, these coefficients differ by no more than a few percent and can be taken equal.

We construct a particle model for the interaction of the two beams, mediated by the medium nonlocality, which allows the beams to interact even if physically non-overlapping. As in the previous section, these mechanical equations are most easily derived from a Lagrangian formulation. The two-color nematicon equations (51)–(53) have the Lagrangian

$$L = i(u^*u_z - uu_z^*) - |\nabla u|^2 + 4\theta|u|^2 + i(v^*v_z - vv_z^*)$$
$$- |\nabla v|^2 + 4\theta|v|^2 - \nu|\nabla\theta|^2 - 2q\theta^2. \tag{54}$$

It was noted in Sec. 2 that there are no known general nematicon solutions for a single beam propagating in a uniform cell. So, we take the general profiles

$$u = a_u f_u\left(\frac{\zeta_u}{w_u}\right)e^{i\sigma_u + iU_u(x-\xi_u) + iV_u(y-\eta_u)}, \quad v = a_v f_v\left(\frac{\zeta_v}{w_v}\right)e^{i\sigma_v + iU_v(x-\xi_v) + iV_v(y-\eta_v)},$$

$$\theta = \alpha_u g_u\left(\frac{\zeta_u}{\beta_u}\right) + \alpha_v g_v\left(\frac{\zeta_v}{\beta_v}\right) \tag{55}$$

for the beams and the NLC response. Here,

$$\zeta_u = \sqrt{(x-\xi_u)^2 + (y-\eta_u)^2}, \quad \zeta_v = \sqrt{(x-\xi_v)^2 + (y-\eta_v)^2}. \tag{56}$$

G. Assanto, P. Panayotaros & N. F. Smyth

The u beam has position (ξ_u, η_u) and velocity (U_u, V_u) and the v beam has position (ξ_v, η_v) and velocity (U_v, V_v). The two beams have angular momentum and, owing to their attractive interaction through the NLC, they can orbit about each other.[18,47–49]

At this point, the high nonlocality allows us to deduce that the beams shed diffractive radiation on a very long z scale as they evolve.[19] Therefore, the mechanical equations governing them, essentially momentum equations, can be found from the (averaged) Lagrangian without modeling the beams' amplitude and width evolutions as the respective total powers $a_u^2 w_u^2$ and $a_v^2 w_v^2$ are essentially conserved.

We substitute the profiles (55) into the Lagrangian (54) and average by integrating in x and y from $-\infty$ to ∞ to result in an averaged Lagrangian $\mathcal{L}$.[15] This averaging process yields various integrals of the beam profiles. While in the previous Sec. 3 these integrals did not arise in the resulting variational (mechanical) equations, here some of them encode the interaction potential between the beams. These involve products of the individual beam profiles and come from the terms $\theta|u|^2$, $\theta|v|^2$, $|\nabla\theta|^2$ and θ^2 in the Lagrangian (54). For these integrals, assumptions about the beam profiles are required and, consistent with the basic hypothesis that diffractive losses can be neglected, we consider that they retain their input Gaussian profiles, i.e.,

$$f_u(r) = f_v(r) = e^{-r^2}. \tag{57}$$

With the assumption (57), the interaction integrals in the averaged Lagrangian are

$$\int_{-\infty}^{\infty}\int_{-\infty}^{\infty} \theta|u|^2 dx dy = \alpha_u a_u^2 w_u^2 I_{12u} + \frac{\alpha_v a_u^2 \beta_v^2 w_u^2}{2(w_u^2 + 2\beta_v^2)} e^{-\rho^2/(w_u^2 + 2\beta_v^2)},$$

$$\int_{-\infty}^{\infty}\int_{-\infty}^{\infty} \theta|v|^2 dx dy = \alpha_v a_v^2 w_v^2 I_{12v} + \frac{\alpha_u a_v^2 \beta_u^2 w_v^2}{2(w_v^2 + 2\beta_u^2)} e^{-\rho^2/(w_v^2 + 2\beta_u^2)},$$

$$\int_{-\infty}^{\infty}\int_{-\infty}^{\infty} |\nabla\theta|^2 dx dy = I_{dpu}\alpha_u^2 + I_{dpv}\alpha_v^2 + \frac{2\alpha_u \alpha_v \beta_u^3 \beta_v^3}{(\beta_u^2 + \beta_v^2)^2}\left[1 - \frac{\rho^2}{\beta_u^2 + \beta_v^2}\right] e^{-\rho^2/(\beta_u^2 + \beta_v^2)},$$

$$\int_{-\infty}^{\infty}\int_{-\infty}^{\infty} \theta^2 dx dy = I_{du2}\alpha_u^2 \beta_u^2 + I_{d2v}\alpha_v^2 \beta_v^2 + \frac{\alpha_u \alpha_v \beta_u^2 \beta_v^2}{\beta_u^2 + \beta_v^2} e^{-\rho^2/(\beta_u^2 + \beta_v^2)}.$$

$$\tag{58}$$

The separation ρ between the beams is given by

$$\rho^2 = (\xi_u - \xi_v)^2 + (\eta_u - \eta_v)^2. \tag{59}$$

"equivalent" variation of the averaged Lagrangian (61) with respect to the velocities (U_u, V_u), (U_v, V_v) and positions (ξ_u, η_u), (ξ_v, η_v) results in the mechanical equations for the two interacting nematicons. To emphasize this connection with mechanics and Newtonian gravitation, we introduce the vector positions of the two nematicons

$\boldsymbol{\xi}_u = (\xi_u, \eta_u)$ and $\boldsymbol{\xi}_v = (\xi_v, \eta_v)$, their vector velocities $\mathbf{V}_u = (U_u, V_u)$ and $\mathbf{V}_v = (U_v, V_v)$ and their relative displacement $\boldsymbol{\rho}$ by

$$\boldsymbol{\rho} = \boldsymbol{\xi}_u - \boldsymbol{\xi}_v. \tag{64}$$

Similarly, we can define the "masses" M_u and M_v (beam powers) by

$$M_u = 2I_{2u}a_u^2 w_u^2, \quad M_v = 2I_{2v}a_v^2 w_v^2. \tag{65}$$

Taking variations of the averaged Lagrangian (61) with respect to ξ_u, ξ_v, η_u, η_v, U_u, U_v, V_u and V_v results in the modulation equations

$$\frac{d}{dz} M_u \mathbf{V}_u = -\left(\frac{\partial \mathcal{P}}{\partial \xi_u}, \frac{\partial \mathcal{P}}{\partial \eta_u}\right), \quad \frac{d}{dz} M_v \mathbf{V}_v = -\left(\frac{\partial \mathcal{P}}{\partial \xi_v}, \frac{\partial \mathcal{P}}{\partial \eta_v}\right) \tag{66}$$

and

$$\frac{d\boldsymbol{\xi}_u}{dz} = \mathbf{V}_u, \quad \frac{d\boldsymbol{\xi}_v}{dz} = \mathbf{V}_v \tag{67}$$

for the two trajectories. It is apparent that these are just Newton's second law cast in terms of equivalent mechanical variables for the nematicons.

These mechanical equations for two interacting nematicons have a close connection with those for the two-body problem from Newtonian gravitation. This can be seen by transforming them into the standard center-of-mass form for the Newtonian Kepler problem. The "center of mass" of the nematicons can be defined as

$$\mathbf{R} = \frac{M_u \boldsymbol{\xi}_u + M_v \boldsymbol{\xi}_v}{M_u + M_v}. \tag{68}$$

In this center-of-mass system, the distance from the origin ρ is defined in (59) and the polar angle is ϕ. Therefore, the system of the two nematicons conserves the angular momentum L_m, with

$$L_m = \rho^2 \frac{d\phi}{dz}. \tag{69}$$

In the center-of-mass coordinates, the mechanical equations (66) and (67) become

$$\frac{d^2\mathbf{R}}{dz^2} = \mathbf{0} \quad \text{and} \quad \frac{d^2\rho}{dz^2} - L_m^2 \rho^{-3} = -\frac{M_u + M_v}{M_u M_v} \frac{\partial \mathcal{P}}{\partial \rho}. \tag{70}$$

Here, $M_u M_v / (M_u + M_v)$ is the "reduced mass" of the system. These are just the standard equations for the Newtonian two-body Kepler problem[50] with the two interacting nematicons resembling two gravitational masses. The equivalent potential (63) has a region of attraction and a minimum, so that there exists a stable orbit for the two nematicons. However, there are fundamental differences between the interaction of two nematicons and of two masses under Newtonian gravitation. Newton's law of gravitation has the force proportional to the product of the two masses, and potential $\mathcal{P} = -GM_u M_v / \rho$. In contrast, the beam parameters and — in particular — the "masses" (65) are tied in to the mechanical momentum equations

G. Assanto, P. Panayotaros & N. F. Smyth

(66) in a nontrivial manner through the potential $\mathcal{P}$ (63), so that the interaction of the nematicons depends in a complicated manner on their parameters (masses), unlike on just the reduced mass as in Newtonian gravitation. Finally, most obviously, the nematicon potential (63) is not the inverse separation potential of Newtonian gravitation, and has both regions of attraction and of repulsion. So, while the interaction of the two nematicons has great similarity to the interaction of two gravitating masses, the actual details are much more involved and the analogy is not complete.

The analogy between interacting nematicons and gravitating masses can be taken further. Among the many exact solutions for gravitating masses, including more than two masses,[51] a classical example is the Lagrange solution for three gravitating masses, for which the configuration is an equilateral triangle. This can be extended to three interacting nematicons, see Ref. 45 for full details. However, due to the form of the nematic potential pinpointed above as compared with the gravitational potential, the equivalent three-nematicon solution does not form an equilateral triangle, but a triangle whose side lengths depend on the individual nematicon powers and the specific parameters in the nematic equations (1) and (2). In addition to the two-body and Lagrange solutions, additional exact gravitation solutions include "figure-8" solutions, as well, but their extension to nematicons is an open question. This is harder because, while the masses in the figure-8 gravitation solution do not collide, this cannot be guaranteed for the nematicon equivalent, due to the more involved potential. Nevertheless, in the light beam case, this is not a reason for the solution to be invalid.

The predictions of the mechanical system (66) and (67) can be compared with numerical solutions of the nematic equations (51)–(53). The latter are solved using a pseudo-spectral method based on the original work in Ref. 52 and extended in Ref. 53 to enhance its stability. The spatial derivatives in (x, y) are evaluated using the Fast Fourier Transform and the beam is propagated in z using the fourth-order Runge–Kutta scheme.

Note that the potential (63) depends on the beam amplitudes and widths a_u, a_v and w_u, w_v and the director (distribution) amplitudes and widths α_u, α_v and β_u, β_v. Consistent with the assumption used to derive the mechanical equations (66) and (67), the beam amplitudes and widths can be taken to retain their input values. However, the amplitudes and widths of the director reorientation are not independent, but determined by the beam through Eq. (53); hence, the director response, or to be more precise an approximation to it, is needed and will be obtained using a variational approximation. As in experiments, we take the input to be Gaussian, so both beam and director response are Gaussian. Hence,

$$f_u(r) = f_v(r) = g_u(r) = g_v(r) = e^{-r^2}. \tag{71}$$

With these profiles, the integrals (60) are

$$I_{2u} = \frac{1}{4}, \quad I_{12u} = \frac{\beta_u^2}{2(w_u^2 + 2\beta_u^2)}, \quad I_{dpu} = \frac{1}{2}, \quad I_{du2} = \frac{1}{4} \tag{72}$$

with symmetric expressions for I_{2v}, I_{12v}, I_{dpv} and I_{dv2}. The values of I_{2pu} and I_{2pv} will not be needed in the following. With these assumptions, the director reorientation for an input beam can be determined from the averaged Lagrangian (61), say for the u beam, by taking $a_v = 0$, $\alpha_v = 0$, $\xi_v = \eta_v = 0$ and $U_v = V_v = 0$. The director distribution for the v beam can be found by symmetry. The averaged Lagrangian required to determine the initial director distributions is then

$$\mathcal{L} = -2I_{2u}a_u^2 w_u^2 \sigma_u' - I_{2pu}a_u^2 + \frac{2\alpha_u a_u^2 w_u^2 \beta_u^2}{w_u^2 + 2\beta_u^2} - \frac{1}{2}\nu\alpha_u^2 - \frac{1}{2}q\alpha_u^2\beta_u^2. \tag{73}$$

Taking variations of this averaged Lagrangian (73) with respect to α_u and β_u gives the input director parameters for the Gaussian profiles (71)

$$\alpha_u = \frac{4a_u^2 w_u^2}{q(w_u^2 + 2\beta_u^2)^2}, \tag{74}$$

$$\beta_u^2 = \frac{1}{4q}[qw_u^2 + (q^2 w_u^4 + 16\nu q w_u^2)^{1/2}] \tag{75}$$

with the v profile found by symmetry. With these expressions for the director parameters the potential (63) can be determined from the input beam, and the mechanical equations (66) and (67) for the interaction of the two nematicons can be solved. These equations are integrated numerically.

Figure 3 shows comparisons for the nematicon trajectory as given by full numerical solutions of the nematic equations (51)–(53) and solutions of the mechanical equations (66) and (67). The comparisons are for the (x, y) beam coordinates (ξ_u, η_u) and (ξ_v, η_v) and the radial positions $r_u^2 = \xi_u^2 + \eta_u^2$ and $r_v^2 = \xi_v^2 + \eta_v^2$. The nonlocality ν was chosen as 500, which is of the order of experimental values.[12] For these initial conditions, the nematicon system has an overall total linear momentum: the two beams' mean trajectory moves according to this mean momentum, while the individual beams oscillate about this mean trajectory and each other. They form a bound state due to the nonlocality,[3,6,18,49] interacting and attracting even at a distance. The agreement between the numerical and mechanical approximation solutions is excellent initially, with differences becoming apparent after $z = 50$, and significant after $z = 150$. After this propagation length, the amplitudes of the oscillations of the beams about the mean are in quite good agreement, but there is a period difference which grows with z. A reason for this is the basic mechanical approximation that the beams retain their power and do not significantly radiate. Figure 4 shows the beams at $z = 0$ and at $z = 300$ for the same parameters as in Fig. 3. Clearly, as the beams evolve, each generates a new, small amplitude beam at the position of the beam in the other mode. Such beams are referred to as shadow beams and are well known to

G. Assanto, P. Panayotaros & N. F. Smyth

result from beam interaction.[54] The powers of these shadow beams are spilled from the main beam, breaking the main hypothesis (beam power conservation) of the mechanical approximation. Hence, deviations of the solutions of the mechanical equations from numerical solutions stem from the generation of shadow beams and their evolution. It may be possible to include these shadow beams in the mechanical beam profile assumption (55), but it will lead to much more involved mechanical equations. This extension may not be possible as the shadow beams start with zero amplitude and are cleft from the main beams; it is not (yet) clear how to break up an initial beam into main and shadow beams in a consistent way.

Figure 5 shows a comparison similar to Fig. 3, but for no overall linear momentum. The beams exhibit no average overall motion, oscillating about $(x, y) = (0, 0)$. The symmetry of the initial condition implies that u and v have the same radial displacements $r_u^2 = \xi_u^2 + \eta_u^2$ and $r_v^2 = \xi_v^2 + \eta_v^2$, which is why in Fig. 5(a) there are only single curves for these variables for the numerical and mechanical solutions of
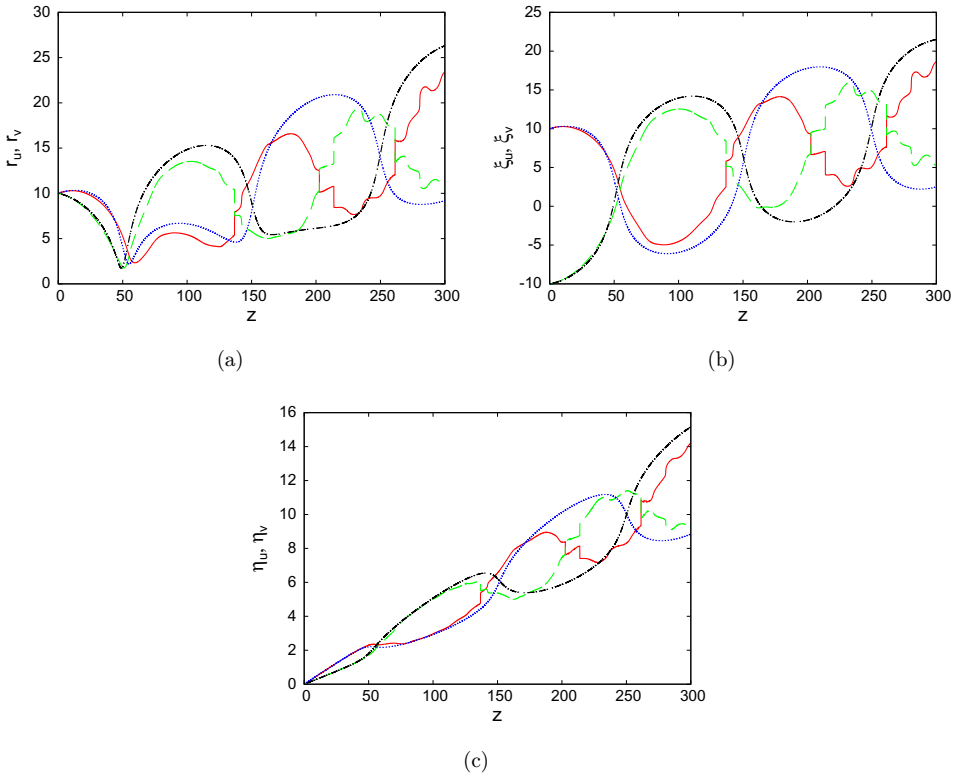

(a)

(b)

(c)

Fig. 3. (Color online) Trajectory comparisons between numerical solutions of system (51)–(53) and solutions of mechanical equations (66) and (67). Numerical solution for u: red (solid) line; numerical solution for v: green (dashed) line; mechanical solution for u: blue (dotted) line; mechanical solution for v: black (dashed-dot) line. (a) radial positions $r_u^2 = \xi_u^2 + \eta_u^2$, $r_v^2 = \xi_v^2 + \eta_v^2$, (b) x positions ξ_u, ξ_v, (c) y positions η_u, η_v. Here the initial beam parameters are $a_u = a_v = 3.0$, $w_u = w_v = 4.5$, $\xi_u = 10.0$, $\xi_v = -10.0$, $\eta_u = \eta_v = 0$, $U_u = V_u = 0.05$, $U_v = V_v = 0.03$. The NLC parameters are $\nu = 500$ and $q = 2$.

both u and v. The same comments for the comparisons in Fig. 3 apply. There is excellent agreement up to about $z = 100$, with significant disagreement after $z = 200$. Again, the agreement for the amplitude of the position oscillations about the mean is quite good, but there is a growing period difference. The overall match between numerical and mechanical solutions is better than for those displayed in Fig. 3, as the numerical solutions for u and v in Fig. 6 show that the shadow beams have much lower amplitude in Fig. 6 than in Fig. 4. Hence, less power is drawn from the main beams to create the shadow beams and, consequently, the main assumption of the mechanical approximation has greater validity. These two examples illustrate advantages and drawbacks of the mechanical approximation discussed in this paper.

It is apparent that the mechanical equations of Sec. 3 for nonuniform samples give better results than those of the present section for interacting nematicons. At variance with the nonuniform orientation case, in fact, in the problem of interacting nematicons the formation of shadow beams had to be considered, together with the Gaussian assumption on beam profiles in order to enable solutions of the mechanical equations to be found. Since the beams will not remain Gaussian as they evolve, assumptions on their profiles reduce the accuracy of the mechanical approximation.
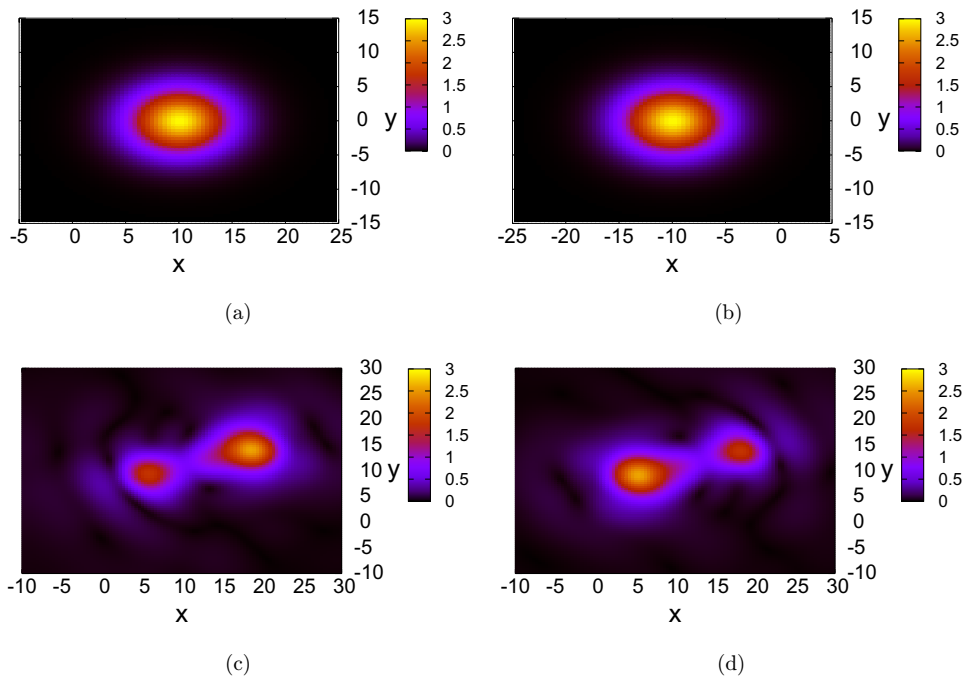

Fig. 4. Numerical solutions of the nematic system (51)–(53). (a) $|u|$ at $z = 0$; (b) $|v|$ at $z = 0$; (c) $|u|$ at $z = 300$; (d) $|v|$ at $z = 300$. Here, the initial beam parameters are $a_u = a_v = 3.0$, $w_u = w_v = 4.5$, $\xi_u = 10.0$, $\xi_v = -10.0$, $\eta_u = \eta_v = 0$, $U_u = V_u = 0.05$, $U_v = V_v = 0.03$. The NLC parameters are $\nu = 500$ and $q = 2$.

5. Energy Minimizing Nematicons and the Regularizing Effect of Nonlocality

Another connection between mechanics and nematicons comes from combining the Hamiltonian mechanics of systems with symmetries and qualitative methods from mathematical analysis. In recent years this approach has been developed extensively for the study of nonlinear waves, see, e.g., Refs. 55–57. In this section we apply these Hamiltonian methods to understand the regularizing effect of nonlocality on solitary wave solutions of the nematic equations (1) and (2), and to address the existence and the stability of nematicons. The next section will discuss nematicon power thresholds and their small amplitude behavior, before finally extending the results to a model that includes saturation of the nonlinearity.

One of the motivations behind these qualitative methods is the question of the existence and multiplicity of solitary wave solutions of nonlinear, dispersive wave equations which lack explicit solutions. For instance, we take the nematic equations
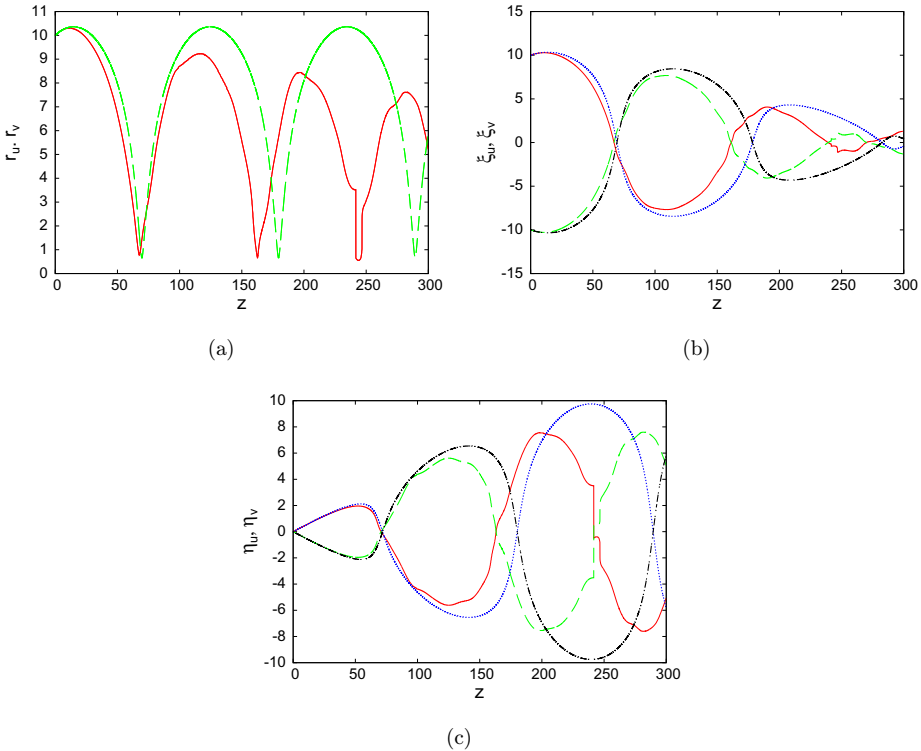

(a)

(b)

(c)

Fig. 5. (Color online) Trajectory comparisons between numerical solutions of the nematic system (51)–(53) and solutions of the mechanical equations (66) and (67). Numerical solution for u: red (solid) line; numerical solution for v: green (dashed) line; mechanical solution for u: blue (dotted) line; mechanical solution for v: black (dashed-dot) line. (a) radial positions $r_u^2 = \xi_u^2 + \eta_u^2$, $r_v^2 = \xi_v^2 + \eta_v^2$, (b) x positions ξ_u, ξ_v, (c) y positions η_u, η_v. Here the initial beam parameters are $a_u = a_v = 3.0$, $w_u = w_v = 4.5$, $\xi_u = 10.0$, $\xi_v = -10.0$, $\eta_u = \eta_v = 0$, $U_u = V_u = 0.05$, $U_v = V_v = -0.05$. The NLC parameters are $\nu = 500$ and $q = 2$.
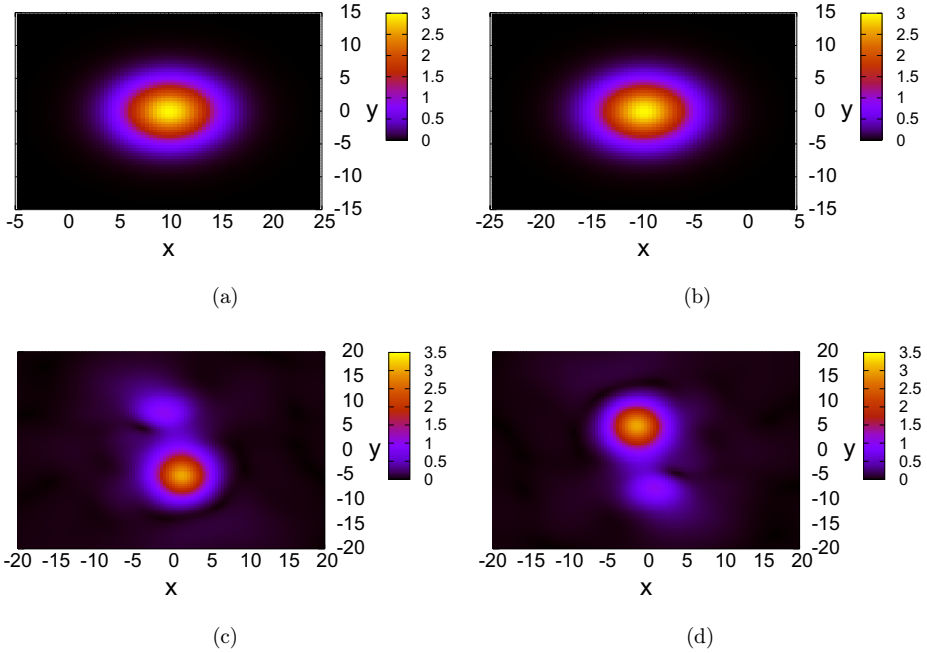
Fig. 6.   Numerical solutions of nematic system (51)–(53). (a) $|u|$ at $z = 0$; (b) $|v|$ at $z = 0$; (c) $|u|$ at $z = 300$; (d) $|v|$ at $z = 300$. The initial beam parameters are $a_u = a_v = 3.0$, $w_u = w_v = 4.5$, $\xi_u = 10.0$, $\xi_v = -10.0$, $\eta_u = \eta_v = 0$, $U_u = V_u = 0.05$, $U_v = V_v = -0.05$. The NLC parameters are $\nu = 500$ and $q = 2$.

(1) and (2) and seek radial solutions of the form $u = f(r)e^{i\sigma z}$ and $\theta = g(r)$, with f real. Then f and g must satisfy the system of ordinary differential equations

$$-\sigma f + \frac{1}{2}\left(\frac{d^2 f}{dr^2} + \frac{1}{r}\frac{df}{dr}\right) + 2fg = 0, \tag{76}$$

$$\nu\left(\frac{d^2 g}{dr^2} + \frac{1}{r}\frac{dg}{dr}\right) - 2qg = -2f^2. \tag{77}$$

We also require differentiability at the origin (i.e., $f'(0) = g'(0) = 0$) and decay at infinity (i.e., $f(r)$ and $g(r)$ both $\to 0$ as $r \to \infty$). The existence of such f and g would show the existence of radially symmetric nematicons. Showing that such solutions exist is, however, nontrivial and has led to rather elaborate theoretical studies. While the more restrictive form assumed for a radial electrical field u and director response θ in (7) led to only one (nondecaying) solution, the approximate methods discussed in Secs. 3 and 4 suggest the existence of more than one decaying solution, e.g., solutions that correspond to experimentally observed nematicons of various powers. In what follows we present results on the existence of radial solutions based on energy minimization arguments that bypass the analysis of the radial equations (76) and (77).

A related question is the stability of nematicons, that is whether a solitary wave solution $u(x, y, z)$ and $\theta(x, y, z)$ obtained from an initial profile that is a small perturbation of a steady nematicon, e.g., the radial profile discussed above, remains close to that profile for all $z > 0$. Unstable solutions depart from the vicinity of the initial profile, resulting in significant distortion. A well known unstable profile is the Townes' solitary wave of cubic Kerr media,[56,58] for which a singularity can occur upon a finite propagation distance z. We show below that nonlocality in NLC prevents such extreme instability for the nematic equations (1) and (2), as pointed out in Ref. 6. In addition, the proof of the existence of nematicon solutions through energy minimization does give partial results on stability.

5.1. *Hamiltonian structure of the nematic equations*

Let us first describe the Hamiltonian structure of the nematic equations (1) and (2). We first solve the medium equation, expressing θ in terms of $|u|^2$ in Fourier space, and obtain

$$\theta(x, y) = \frac{2}{\nu} \int_{\mathbf{R}^2} K_0(m\sqrt{(x - \eta)^2 + (y - \xi)^2})|u(\eta, \xi)|^2 d\xi d\eta, \tag{78}$$

where K_0 is the modified Bessel function[59] and $m = \sqrt{2q/\nu}$. The Bessel function $K_0(r)$, defined for $r > 0$, is positive and strictly decreasing; it satisfies

$$K_0(r) = \frac{1}{2\pi}\left(-\log r + (\log 2 - \gamma)\right) + O(r^2) \quad \text{as } r \to 0 \tag{79}$$

and

$$K_0(r) = \frac{1}{2\sqrt{2\pi r}} e^{-r}(1 + O(r^{-1})) \quad \text{as } r \to \infty, \tag{80}$$

with γ the Euler–Mascheroni constant.[59] We note that the logarithmic singularity at the origin is integrable on the plane.

Denoting the convolution of two functions f and g on the plane as

$$(f * g)(x_1, x_2) = \int_{\mathbf{R}^2} f(x_1 - y_1, x_2 - y_2)g(y_1, y_2)dy_1 dy_2 \tag{81}$$

and writing the nematic response as $\theta = G(|u|^2) = \frac{2}{\nu} K_{0,m} * |u|^2, K_{0,m}(r) = K_0(mr)$, with G defined as in the medium response solution (78), the electric field equation (1) becomes

$$iu_z + \frac{1}{2} \nabla^2 u + 2G(|u|^2)u = 0. \tag{82}$$

Equation (82) can be written as Hamilton's equation

$$u_z = -i\frac{\delta H}{\delta u^*}, \quad \text{with } H = \int_{\mathbf{R}^2} \left(\frac{1}{2}|\nabla u|^2 - |u|^2 G(|u|^2)\right), \tag{83}$$

where H is the *Hamiltonian* or *energy* of Eq. (82).[56,57,60] The variational derivatives

$\frac{\delta H}{\delta u^*}$ and $\frac{\delta H}{\delta u}$ are defined implicitly by the expansion of $H(u + u_1)$, assuming that u_1 is a small perturbation of u, as

$$H(u + u_1) = H(u) + \int_{\mathbf{R}^2} \frac{\delta H}{\delta u^*} u_1^* + \int_{\mathbf{R}^2} \frac{\delta H}{\delta u} u_1 + O(u_1^2) \tag{84}$$

and the superscript * denotes the complex conjugate. To obtain this expression we separated the part of $H(u + u_1)$ that is linear in u_1 and u_1^* and then identified the structure above, in analogy to the Taylor expansion of a scalar function in $\mathbf{R}^n$, e.g., $h(x + y) = h(x) + \nabla h(x) \cdot y + O(y^2)$. The Hamiltonian formulation of the electric field equation Eq. (82) of the electric field equation implies the conservation of H. Another conserved quantity is the power P, defined as

$$P(u) = \int_{\mathbf{R}^2} |u|^2. \tag{85}$$

The conservation of P is related by Nöther's theorem to the fact that the Hamiltonian is invariant under the global phase change $u(x, y) \to e^{i\phi} u(x, y)$, with ϕ independent of (x, y). Other conserved quantities and symmetries of the electric field equation (82) are discussed in Refs. 56 and 57.

NLS-type equations of the form (82), with $G(|u|^2) = F * |u|^2$ the convolution of $|u|^2$ with a radially dependent kernel F, have been considered in several contexts and are usually referred to as nonlinearities of Hartree type, see, e.g., models with kernels that avoid the singularity of the Bessel function K_0 at the origin.[61,62] The Hamiltonian structure requires the symmetry of the operator G, and this is guaranteed if F is radial. The Hamiltonian in these models can be also directly derived from a Lagrangian similar to the ones used in Secs. 3 and 4. The connection between the two functionals, Hamiltonians and Lagrangians, is well known in mechanics and field theory. Nevertheless, their uses are quite different in this paper.

5.2. *Energy conservation and the regularizing effect of nonlocality*

We can use the conservations of energy and power to demonstrate the regularizing effect of the nonlocality of the nematic response.[6] The main results are implicit in the work of Ginibre and Velo,[63] who studied Hartee-type NLS equations with a general class of kernels. Their theory, in fact, includes the $(2 + 1)$D nematic equations (1) and (2).[64] The general idea is to use conservation of energy and show that $\int_{\mathbf{R}^2} |\nabla u|^2$ remains bounded. We observe that the (focusing) sign combination in the electric field equation (83) allows both the quadratic and quartic terms of H to increase without bound, but keeping their difference constant. Thus, to exploit conservation of energy we first need to somehow connect the quadratic and quartic parts and correlate their rates of growth.

Note that if $\int_{\mathbf{R}^2} |\nabla u|^2$ remains bounded, then

$$\left[\int_{\mathbf{R}^2} (|u(x, y)|^2 + |\nabla u(x, y)|^2) dx dy \right]^{1/2} \tag{86}$$

G. Assanto, P. Panayotaros & N. F. Smyth

remains bounded as well. The latter is referred to as the H^1 norm of u. We can define the space H^1 of functions as the set of differentiable functions (and their suitable limits) of finite H^1 norm.[65] The H^1 norm of u is also given by

$$\left[\int_{\mathbf{R}^2}(1+k_1^2+k_2^2)|\hat{u}(k_1,k_2)|^2 dk_1 dk_2\right]^{1/2}, \tag{87}$$

where $\hat{u}(k_1,k_2)$ is the Fourier transform of u.[55] The fact that the H^1 norm remains bounded provides a worst case scenario for the decay of the Fourier transform of solutions, valid for all z. Most importantly in nonlinear optics, singularity formation for solutions of the $(2+1)$D cubic NLS equation is accompanied by the divergence of the H^1 norm in finite z.[58] Therefore, the control of this quantity is important and preliminary for more precise results on the behavior of solutions of the nematic equations.

To ascertain the role of nonlocality on solutions of the $(2+1)$D nematic equations we can exploit an argument by Turytsin.[66] First, we note that, the quartic part of the energy $\int_{\mathbf{R}^2} G(|u|^2)|u|^2$ can be bounded as

$$\int_{\mathbf{R}^2}(K_{0,m}*|u|^2)(\mathbf{x})|u(\mathbf{x})|^2 d^2\mathbf{x} \leq \left(\sup_{\mathbf{x}\in\mathbf{R}^2}|(K_{0,m}*|u|^2)(\mathbf{x})|\right)\int_{\mathbf{R}^2}|u(\mathbf{x})|^2 d^2\mathbf{x}, \tag{88}$$

with $\mathbf{x}=[x,y]$. The integral on the right-hand side is the optical power $P(u)$, a constant of motion. To estimate the integral on the left-hand side and check that it is indeed finite, we observe that

$$\left|\int_{\mathbf{R}^2}K_{0,m}(|\mathbf{x}-\mathbf{x}'|)\frac{|\mathbf{x}-\mathbf{x}'|}{|\mathbf{x}-\mathbf{x}'|}|u(\mathbf{x}')|^2 d^2\mathbf{x}'\right| \leq \left(\max_{\mathbf{x}'\in\mathbf{R}^2}|\mathbf{x}-\mathbf{x}'|K_{0,m}(|\mathbf{x}-\mathbf{x}'|)\right)$$
$$\times\int_{\mathbf{R}^2}\frac{|u(\mathbf{x}')|^2}{|\mathbf{x}-\mathbf{x}'|}d^2\mathbf{x}'. \tag{89}$$

The quantity in parentheses on the right-hand side is finite by the asymptotic results (79) and (80) for the Bessel function K_0 at the origin and at infinity, respectively. To bound the integral on the right-hand side, we point out that the singularity at $\mathbf{x}'=\mathbf{x}$ is integrable on the plane. The integral is then finite if u is differentiable and has a sufficiently rapid decay. To estimate this, we start by using that

$$\int_{\mathbf{R}^2}\nabla u(\mathbf{x})\cdot\frac{u^*(\mathbf{x})(\mathbf{x}-\mathbf{x}')}{|\mathbf{x}-\mathbf{x}'|}d^2\mathbf{x} = -\int_{\mathbf{R}^2}u(\mathbf{x})\cdot\nabla\cdot\frac{u^*(\mathbf{x})(\mathbf{x}-\mathbf{x}')}{|\mathbf{x}-\mathbf{x}'|}d^2\mathbf{x} \tag{90}$$

on integrating by parts. Then

$$2\int_{\mathbf{R}^2}\nabla u(\mathbf{x})\cdot\frac{u^*(\mathbf{x})(\mathbf{x}-\mathbf{x}')}{|\mathbf{x}-\mathbf{x}'|}d^2\mathbf{x} = -\int_{\mathbf{R}^2}|u(\mathbf{x})|^2\cdot\nabla\frac{(\mathbf{x}-\mathbf{x}')}{|\mathbf{x}-\mathbf{x}'|}d^2\mathbf{x}$$
$$= -\int_{\mathbf{R}^2}\frac{|u(\mathbf{x})|^2}{|\mathbf{x}-\mathbf{x}'|}d^2\mathbf{x}. \tag{91}$$

Thus the second integral of Eq. (89) satisfies

$$\int_{\mathbf{R}^2} \frac{|u(\mathbf{x})|^2}{|\mathbf{x}-\mathbf{x}'|} d^2\mathbf{x} \le 2 \int_{\mathbf{R}^2} |\nabla u(\mathbf{x})||u(\mathbf{x})| d^2\mathbf{x} \le 2 \left(\int_{\mathbf{R}^2} |\nabla u(\mathbf{x})|^2 d^2\mathbf{x} \right)^{1/2}$$
$$\times \left(\int_{\mathbf{R}^2} |u(\mathbf{x})|^2 d^2\mathbf{x} \right)^{1/2}, \tag{92}$$

by means of the inequalities $\int f g^* \le (\int |f|^2)^{1/2} (\int |g|^2)^{1/2}$ (Cauchy–Schwartz inequality) and $|\int f| \le \int |f|$. The second integral is $\sqrt{P(u)}$, a constant. Collecting the bounds (88), (89) and (92) we see that the quartic part of the energy satisfies

$$\int_{\mathbf{R}^2} (K_{0,m} * |u|^2)(\mathbf{x})|u(\mathbf{x})|^2 d^2\mathbf{x} \le 2MP^{3/2}(u) \left(\int_{\mathbf{R}^2} |\nabla u(\mathbf{x})|^2 d^2\mathbf{x} \right)^{1/2}. \tag{93}$$

This estimate involves the quantities appearing in the H^1 norm (which allows us to extend it to all H^1 functions by taking limits of the smooth and rapidly decaying functions, as assumed in the previous steps). Combining (93) with (83), we obtain

$$H \ge \frac{1}{2} \int_{\mathbf{R}^2} |\nabla u|^2 - \frac{4}{\nu} MP^2(u) \left(\int_{\mathbf{R}^2} |\nabla u|^2 \right)^{1/2}. \tag{94}$$

Since the optical power $P(u)$ is constant, if $\int_{\mathbf{R}^2} |\nabla u|^2$ diverges, then H must also diverge, contradicting the conservation of energy. Therefore, $\int_{\mathbf{R}^2} |\nabla u|^2$ must remain bounded for all z. While a variant of this argument was used in Ref. 61 for kernels with an absolutely integrable Fourier transform, e.g., for Gaussians (but not for $\hat{K}_0$), it will not work for the $(2+1)$D NLS equation for a Kerr medium (cubic nonlinearity). Note that, the nonlinear part of the energy for power and Hartree nonlinearities can be estimated in a general way using the Gagliardo–Nirenberg inequalities,[63,67] which bound integrals of powers of a function u by the product of an integral of some power of $|u|$ and an integral of some power of $|\nabla u|$.[55,65] For the Hamiltonian of the cubic NLS equation in Kerr media (focusing case) we have

$$H_\sigma = \int_{\mathbf{R}^2} (|\nabla u|^2 - |u|^4) \tag{95}$$

and also the Gagliardo–Nirenberg inequality

$$\int_{\mathbf{R}^2} |u|^4 \le C_{2,2} \left(\int_{\mathbf{R}^2} |u|^2 \right)^\alpha \left(\int_{\mathbf{R}^2} |\nabla u|^2 \right)^\beta, \tag{96}$$

with $\alpha = \beta = 2$ and $C_{2,2}$ a positive constant. The exponents α and β are determined uniquely by a scaling argument. Then

$$H_\sigma(u) \ge \int_{\mathbf{R}^2} |\nabla u|^2 - C_{2,2} P(u) \int_{\mathbf{R}^2} |\nabla u|^2. \tag{97}$$

For $P(u) < 1/C_{2,2}$, the divergence of $\int_{\mathbf{R}^2} |\nabla u|^2$ leads to an unbounded growth of the left-hand side of (97), contradicting energy conservation. Therefore, a small power leads to a bound on $\int_{\mathbf{R}^2} |\nabla u|^2$. This argument does not work for $P(u) \geq 1/C_{2,2}$, where in fact $\int_{\mathbf{R}^2} |\nabla u|^2$ can diverge over a finite distance z.[56–58] The regularizing effect of nonlocality is therefore related to the slower growth of the quartic energy in $\int_{\mathbf{R}^2} |\nabla u|^2$, as seen by comparing (93) to (97).

6. Energy Minimizing Nematicons and Power Thresholds

Another application of the Hamiltonian structure of the nematic equations (1) and (2) is a result on the existence of solutions $u(x, y, z) = \psi(x, y)e^{i\sigma z}$ that minimize the energy (Hamiltonian H) over all functions in the space H^1 (see comments below) of constant power P. We argue that these solutions should correspond to experimentally observed nematicons.

Substituting the solitary wave form $u(x, y, z) = \psi(x, y)e^{i\sigma z}$ in the electric field equation (82) leads to

$$\sigma\psi = -\frac{1}{2}\Delta\psi - 2\psi G(|\psi|^2). \tag{98}$$

By the Hamiltonian formulation (83) and (84) this is also equivalent to

$$\sigma\frac{\delta P}{\delta u^*}(\psi) = \frac{\delta H}{\delta u^*}(\psi), \tag{99}$$

i.e., we have the variational derivatives of P and H evaluated at $u = \psi$. Thus, ψ is a critical point of the Hamiltonian H over functions of constant power P with the frequency σ playing the role of a Lagrange multiplier. It was proven in Ref. 64 that there exist a real number $c_0 > 0$ and a complex valued function ψ_c on the plane that minimizes the Hamiltonian $H(v)$ over all complex valued functions v on the plane satisfying $P(v) = c$, $c > c_0$, and belonging to H^1. Even though the appearance of the function space H^1 is just a technical part of the proof, this a large set of functions, including — for instance — all differentiable u with finite H^1 norm. According to (86) this is a mild condition on decay at infinity, slightly stronger than requiring finite power. Moreover, the regularization arguments above for the nematic equations imply that initial conditions in H^1 remain in H^1 for all z and have a bounded H^1 norm. This set of functions is therefore a natural choice for examining detailed features of the nematic equations.

A second result is that a minimum ψ_c of the energy H over H^1 functions of constant power $P = c$ is, up to translation and global phase changes, a smooth, radial, real and positive solution of (98), that also decays monotonically to zero at infinity,[64] as for experimentally observed nematicons. The minima of H at fixed power are also expected to be stable, and thus observable. This is because an initial profile near ψ_c that becomes significantly distorted, i.e., leaves the vicinity of ψ_c, can only have higher energy H and so contradict the conservation of H.[64] These

properties of radial symmetry, monotonic decay to zero and stability suggest that an energy minimizer ψ_c corresponds to an experimentally observed (or observable) nematicon. Two open questions of physical relevance are (i) whether radial functions of minimal energy at fixed power are unique and (ii) whether other local minima of H (i.e., configurations of higher energy) exist at fixed power. Multiple local minima would imply the existence of other possible stable nematicon solutions.

We now turn our attention to the fact that the existence of energy minimizing nematicons at a fixed power was shown for powers above a certain threshold λ_0. Physically, this suggests that nematicons cannot be observed for arbitrarily small powers. The analysis in Ref. 64 led to theoretical predictions for this minimum power. The main observation towards the power threshold is that the existence of H^1 functions minimising H at a given power $P = \lambda$ requires the existence of configurations with negative values of H. Intuitively, this is needed to rule out the possibility of making the energy decrease to zero by considering a sequence of profiles with decreasing and vanishing amplitude (and constant power). Such a sequence of configurations would lead to a vanishing energy without converging, i.e., without reaching a specific profile that minimizes the energy. Requiring profiles of negative energy H at power $P = \lambda$ yields a condition $\lambda > \lambda_0$. We can estimate the threshold power λ_0 by using trial functions: we can consider a radial trial function $v(r) = af(\frac{r}{s})$ (in H^1) and vary the parameters a and $s > 0$ to make $H(v) < 0$, keeping the power $P(v)$ constant. We compute

$$H = \lambda(\mathcal{A} - \mathcal{B}\lambda), \quad \mathcal{A} = \frac{1}{2}\frac{I_{22}}{4s^2 I_2}, \quad \mathcal{B} = \frac{1}{2\pi}\frac{I_4(s)}{I_2^2}, \tag{100}$$

where

$$I_2 = \int_0^\infty rf^2(r)dr, \quad I_{22} = \int_0^\infty r(f'(r))^2 dr, \tag{101}$$

$$I_4(s) = \int_0^\infty \int_0^\infty I(sr_1, sr_2)r_1 r_2 f^2(r_1)f^2(r_2)dr_1 dr_2, \tag{102}$$

$$I(sr_1, sr_2) = 2\int_0^\pi K_0(sm(r_1^2 + r_2^2 - 2r_1 r_2 \cos\theta)^{1/2})d\theta. \tag{103}$$

Fixing s, the integrals I_2 and I_{22} are positive constants and, by the positivity of the Bessel function K_0, $I_4(s)$ is also a positive constant. Using the results (100), we have that $H(v) < 0$ if

$$\lambda > \frac{\mathcal{A}}{\mathcal{B}} = \frac{\pi}{2}\frac{I_2 I_{22}}{s^2 I_4(s)}. \tag{104}$$

The quantity $\mathcal{A}/\mathcal{B}$ can be computed numerically and used as an approximation for the minimum power needed to support a nematicon. This is reasonable, provided $v(r) = af(r/s)$, with a real, is a good approximation to the exact nematicon profile. At the same time, we may be able to find f and s leading to a smaller $\mathcal{A}/\mathcal{B}$. The

question is then whether this ratio can be made arbitrarily close to zero by choosing a suitable sequence of trial functions that would entail the existence of nematicons with arbitrarily small powers. It was shown in Ref. 64 that $\mathcal{A}/\mathcal{B}$ can be made independent of the choice of trial function, as follows from the inequality

$$s^2 I_4(s) \le C I_2 I_{22}, \tag{105}$$

valid for all $f \in H^1$ and real s, i.e., with C independent of f and s. Through (104), the inequality (105) implies that for

$$\lambda > \lambda_0 = \frac{\pi}{2C} \tag{106}$$

the energy H of H^1 radial solutions of power $P = \lambda$ can attain negative values. The latter implies the existence of an energy minimizing nematicon.

From a physical point of view, the minimum power result Eq. (106) is an interesting theoretical prediction of the threshold for the formation of nematicons. Mathematically the power bound (106) is a sufficient condition for the existence of energy minimizing nematicons. On the other hand, all initial profiles (in H^1) of sufficiently small power must eventually diffract as $z \to \infty$,[64] implying that we cannot have nematicons of arbitrarily small powers. A similar diffraction result for small powers is also valid for the standard NLS model of a Kerr medium in $(2+1)$ dimensions.[25]

The result on diffraction for small optical powers also has implications for the numerical computation of nematicons. A commonly used technique to find nematicon solutions uses energy minimization at fixed power, considering suitable discretizations of the Hamiltonian H and the power P for functions defined on a finite computational grid.[64] The discrete analogue of the power constraint $P = c$ is a sphere of radius c in a finite dimensional space. The discretization of H, restricted to this sphere, always has a minimum for any $c > 0$, at variance with the theoretical continuous result of eventual decay for small enough power. Such numerical solutions are spurious and are, in essence, a finite domain effect, i.e., not due to the discretization. For instance, power thresholds for discrete analogues of solitary waves and decay for small power are also known for the discrete cubic NLS equation on an infinite two dimensional lattice.[68,69]

We stress that these threshold and small power decay results refer to equations defined on the infinite plane. The implications for a realistic experimental, i.e., finite, geometry, are that an initially localized beam of sufficiently small power will start diffracting, as predicted by the infinite domain model.[70]

Finally, the dimensionality of the model also plays a role. We expect that the $(1+1)$-dimensional nematic system does not have a power threshold for solitary waves. Thus, $(1+1)$D models are useful approximations, but may miss small power effects.

6.1. *Extensions to saturable model*

As discussed in the previous sections, the nematic system (1) and (2) is an approximation to a full system with a saturable nonlinearity that can be traced back to the coupled Maxwell–Oseen–Frank model for light beams propagating in nematic liquid crystals.[40] A saturating nonlinear response is quite intuitive, considering that the molecular director can — at the most — align with the polarization of the electric field of the light beam. However, fewer studies have dealt with the combination of saturation and nonlocality in NLC. We look here at the model

$$i\partial_z u + \frac{1}{2}\nabla^2 u + u\sin(2\theta) = 0 \qquad (107)$$

for the electric field of the beam and

$$\nu\nabla^2\theta - q\sin(2\theta) = -2|u|^2\cos(2\theta) \qquad (108)$$

for the optically induced rotation θ of the molecular director.[71] Here, ν is the non-dimensional elasticity of the nematic medium and q is a positive constant proportional to the square of the external electric field which pre-sets the NLC molecules in the principal plane (x,z).[3,5]

The nematic equations (1) and (2) are obtained from the more general equations (107) and (108) on assuming that the light induced rotation θ is small and Taylor expanding $\sin\theta$ and $\cos\theta$ to first order. We note that, in the local limit $\nu = 0$, the director equation (108) yields $\tan 2\theta = 2|u|^2/q$, so that the electric field equation (107) becomes

$$i\partial_z u + \frac{1}{2}\nabla^2 u + \frac{2|u|^2 u}{\sqrt{q^2 + 4|u|^4}} = 0, \qquad (109)$$

which is a saturable NLS equation.[25] This suggests an additional regularizing mechanism of the nematic equations (107) and (108) in $(2+1)$ dimensions,[5] as saturation prevents catastrophic collapse upon self-focusing.[25]

A more precise way to verify this is indeed the case stems from the fact that the energy

$$H_s = \frac{1}{4}\int_{\mathbf{R}^2}\left(|\nabla u|^2 + \nu|\nabla\theta|^2 - 2|u|^2\sin(2\theta) + q(1-\cos(2\theta))\right) \qquad (110)$$

is conserved under the evolution governed by the nematic equations (107) and (108), with H_s the Hamiltonian. In particular, we can cast the system (107) and (108) in the form

$$u_z = -i\frac{\delta H_s}{\delta u^*}, \quad \frac{\delta H_s}{\delta\theta} = 0 \qquad (111)$$

with $H_s = H_s(u, u^*, \theta)$. This is a generalization of the Hamiltonian structure, leading automatically to the conservation of (the energy) H_s. The power $P(u)$, defined as in

(85), is also conserved. From the Hamiltonian (110) we have

$$H_s \geq \frac{1}{4} \int_{\mathbf{R}^2} (|\nabla u|^2 - |u|^2 \sin \theta), \tag{112}$$

i.e., on omitting the positive terms of H_s (which are finite[71]),

$$\int_{\mathbf{R}^2} |u|^2 \sin \theta \leq \int_{\mathbf{R}^2} |u|^2 |\sin \theta| \leq P(u). \tag{113}$$

Therefore,

$$H_s \geq \frac{1}{4} \int_{\mathbf{R}^2} \left[|\nabla u|^2 - \frac{1}{4} P(u) \right]. \tag{114}$$

By the conservation of the power P, if $\int_{\mathbf{R}^2} |\nabla u|^2$ diverges, then H_s must also diverge, contradicting conservation of energy. We thus have a much simpler variant of the argument used above to control the H^1 norm of the nematicon solution of the simplified nematic equations (1) and (2). In the present saturable model, the part of the Hamiltonian leading to the nonlinear coupling of u and θ has a much milder growth in u and is controlled by the power. This is a manifestation of the saturation of the nonlinearity at larger angles θ.

The analysis of the director equation (108) shows that there is a unique solution $\theta = G(|u|^2)$.[71] An interesting result is that θ is positive everywhere and also satisfies an upper bound $\theta(\mathbf{x}) \leq \theta_{\max}$ for all $\mathbf{x} = (x, y)$ on the plane, i.e., the angle saturates.

In the simplified nematicon model (1) and (2), a positive θ follows from the Green's function solution (78) and the positivity of the Bessel function kernel K_0. The positivity of θ in the saturable model (107) and (108) makes the director equations of the two models consistent at small angles. The saturation result for (108) is an indication of the physical consistency of the saturable system at larger angles, as saturation is expected by the configuration of the field-dipole (director) interaction.[3,5] It also improves the director equation (2), for which the linearity of $\theta = \frac{2}{\nu} K_{0,m} * |u|^2$ implies that θ can be arbitrarily large.

By minimizing the Hamiltonian $H_s(v, \theta)$ over configurations of v and θ of fixed power $P(v) = c$ (v and θ are assumed to be H^1 functions), the existence of a solitary wave solution $u(x, y, z) = v(x, y)e^{i\sigma z}$ of the saturable nematic equations (107) and (108) can be proven. Provided its power is above a threshold, this energy minimizing solitary wave can be shown to exist, to be stable and to exhibit a positive radial profile that decays monotonically to zero (up to phase changes and position translations).[71] Moreover, initial profiles of small enough power eventually diffract. Therefore, the saturable nematic model has a stable "saturable nematicon" solution with the qualitative properties of the nematicon described by the linearized equations (1) and (2) and by experimental measurements.[3]

Finally, the saturable equations (107) and (108) confirm and extend the results on existence and basic properties of nematicons based on the simplified equations (1)

and (2), adding the beneficial effect of saturation of the director orientation for large fields and regularizing the solution. The two models are expected to give similar results for small and intermediate power levels, i.e., below and immediately above the threshold for nematicon formation; they should diverge for higher excitations. Nevertheless, higher powers are likely to introduce physical effects not modeled by Hamiltonian systems.

7. Conclusions

While nonlinear optics often appears far removed from classical mechanics, Lagrangian and Hamiltonian ideas and techniques well known in areas ranging in length scale from astronomy to micromanipulation can be exploited to analyze beam self-localization in nonlinear, nonlocal optical media such as nematic liquid crystals. This is because optical solitary waves in these materials behave in many aspects as particles.[16] In this Review we have exploited the analogy of nematicons with mechanical particles in a potential to bypass the lack of known exact nematicon solutions of the nematic equations. Mechanical counterpart equations to those describing nematicons have been employed, resorting to momentum conservation to model and describe single solitary waves evolving in nonuniform NLC samples with transverse or longitudinal modulation of the background orientation, as well as two or three interacting nematicons in homogeneous samples. In most cases, the agreement between the mechanical model, experimental observations and the results of realistic numerical integration was found to be excellent, despite assumptions on lossless material and propagation, as well as other simplifying approximations. Moreover, we have shown that analogies with Hamiltonian mechanics for systems with symmetries lead to arguments on the existence, uniqueness and stability of nematicon solutions, emphasizing the regularization afforded by nonlocality and saturation of the NLC nonlinear response and showing important implications for the link between the actual solutions of the (continuous) nematic equations and their discrete version in numerical schemes. The latter can yield spurious results if not used with caution, as should be more widely appreciated. Finally, the existence of a power threshold for nematicons, their eventual diffraction for low excitations and their observability for various input powers are among the beneficial results stemming from the combination of Hamiltonian mechanics and related mathematical methods. While mathematical modeling of nematicons in nonlinear, nonlocal and saturable nematic liquid crystals has achieved substantial progress using these mechanical analogies, further work needs to be carried out to model more involved interactions and/or the interplay of various nonlinear responses in NLC, including, e.g., symmetry breaking and bistability,[72,73] interplay/competition of thermo-optic and reorientational phenomena,[9,41–43,74] coexistence of electronic and reorientational responses acting on different time scales,[75–77] reorientation in the presence of geometric phases,[78,79] synergy of optical gain and scattering in doped NLC[80–82] and more.

G. Assanto, P. Panayotaros & N. F. Smyth

References

1. I. C. Khoo, Nonlinear optics of liquid crystalline materials, *Phys. Rep.* **471** (2009) 221–267.

2. A. Alberucci, A. Piccardi, M. Peccianti, M. Kaczmarek and G. Assanto, Propagation of spatial optical solitons in a dielectric with adjustable nonlinearity, *Phys. Rev. A* **82** (2010) 023806.

3. M. Peccianti and G. Assanto, Nematicons, *Phys. Rep.* **516** (2012) 147–208.

4. G. Assanto, *Nematicons, Spatial Optical Solitons in Nematic Liquid Crystals* (John Wiley and Sons, New York, 2012).

5. M. Peccianti, A. De Rossi, G. Assanto, A. De Luca, C. Umeton and I. C. Khoo, Electrically assisted self-confinement and waveguiding in planar nematic liquid crystal cells, *Appl. Phys. Lett.* **77** (2000) 7–9.

6. C. Conti, M. Peccianti and G. Assanto, Route to nonlocality and observation of accessible solitons, *Phys. Rev. Lett.* **91** (2003) 073901.

7. M. Peccianti, C. Conti, G. Assanto, A. De Luca and C. Umeton, Nonlocal optical propagation in nonlinear nematic liquid crystals, *J. Nonl. Opt. Phys. Mat.* **12** (2003) 525–538.

8. M. Peccianti, C. Conti, G. Assanto, A. De Luca and C. Umeton, Routing of anisotropic spatial solitons and modulational instability in liquid crystals, *Nature* **432** (2004) 733–737.

9. U. A. Laudyn, M. Kwasny, A. Piccardi, M. Karpierz, R. Dabrowski, O. Chojnowska, A. Alberucci and G. Assanto, Nonlinear competition in nematicon propagation, *Opt. Lett.* **40** (2015) 5235–5238.

10. U. A. Laudyn, M. Kwaśny, F. A. Sala, M. A. Karpierz, N. F. Smyth and G. Assanto, Curved optical solitons subject to transverse acceleration in reorientational soft matter, *Sci. Rep.* **7** (2017) 12385.

11. U. A. Laudyn, M. Kwaśny, M. Karpierz, N. F. Smyth and G. Assanto, Accelerated optical solitons in reorientational media with transverse invariance and longitudinally modulated birefringence, *Phys. Rev. A* **98** (2018) 023810.

12. G. Assanto, A. A. Minzoni, M. Peccianti and N. F. Smyth, Optical solitary waves escaping a wide trapping potential in nematic liquid crystals: Modulation theory, *Phys. Rev. A* **79** (2009) 033837.

13. Y. Izdebskaya, W. Krolikowski, N. F. Smyth and G. Assanto, Vortex stabilization by means of spatial solitons in nonlocal media, *J. Opt.* **18** (2016) 054006.

14. J. M. L. MacNeil, N. F. Smyth and G. Assanto, Exact and approximate solutions for solitary waves in nematic liquid crystals, *Physica D* **284** (2014) 1–15.

15. G. B. Whitham, *Linear and Nonlinear Waves* (J. Wiley and Sons, New York, 1974).

16. D. J. Kaup and A. C. Newell, Solitons as particles, oscillators, and in slowly changing media: A singular perturbation theory, *Proc. Roy. Soc. Lond. A* **361** (1978) 413–446.

17. A. B. Aceves, J. V. Moloney and A. C. Newell, Theory of light-beam propagation at nonlinear interfaces. I Equivalent-particle theory for a single interface, *Phys. Rev. A* **39** (1989) 1809–1827.

18. G. Assanto, N. F. Smyth and A. L. Worthy, Two colour, nonlocal vector solitary waves with angular momentum in nematic liquid crystals, *Phys. Rev. A* **78** (2008) 013832.

19. B. D. Skuse and N. F. Smyth, Interaction of two colour solitary waves in a liquid crystal in the nonlocal regime, *Phys. Rev. A* **79** (2009) 063806.

20. G. Assanto, A. A. Minzoni and N. F. Smyth, Light self-localization in nematic liquid crystals: Modelling solitons in nonlocal reorientational media, *J. Nonlin. Opt. Phys. Mater.* **18** (2009) 657–691.

21. S. Zheng, M. Chen, T. Zheng, W. Hu, Q. Guo and D. Lu, Analytical modelling of soliton interactions in a nonlocal nonlinear medium analogous to gravitational force, *Phys. Rev. A* **97** (2018) 013817.

22. F. A. Sala, N. F. Smyth, U. A. Laudyn, M. A. Karpierz, A. A. Minzoni and G. Assanto, Bending reorientational solitons with modulated alignment, *J. Opt. Soc. Amer. B* **34** (2017) 2459–2466.

23. B. Malomed, Variational methods in nonlinear fiber optics and related fields, *Prog. Opt.* **43** (2002) 71–193.

24. A. C. Newell, *Solitons in Mathematics and Physics* (SIAM, Philadelphia, 1985).

25. Y. S. Kivshar and G. P. Agrawal, *Optical Solitons. From Fibers to Photonic Crystals* (Academic Press, San Diego, 2003).

26. G. I. Stegeman, G. Assanto, R. Zanoni, C. T. Seaton, E. Garmire, A. A. Maradudin, R. Reinisch and G. Vitrant, Bistability and switching in nonlinear prism coupling, *Appl. Phys. Lett.* **52** (1988) 869–871.

27. G. Vitrant, R. Reinisch, J. Cl. Paumier, G. Assanto and G. I. Stegeman, Non-linear prism coupling with nonlocality, *Opt. Lett.* **14** (1989) 898–890.

28. S. Skupin, M. Saffman and W. Krolikowski, Nonlocal stabilization of nonlinear beams in a self-focusing atomic vapor, *Phys. Rev. Lett.* **98** (2007) 263902.

29. C. Rotschild, O. Cohen, O. Manela, M. Segev and T. Carmon, Solitons in nonlinear media with an infinite range of nonlocality: First observation of coherent elliptic solitons and of vortex-ring solitons, *Phys. Rev. Lett.* **95** (2005) 213904.

30. S. Skupin, O. Bang, D. Edmundson and W. Krolikowski, Stability of two-dimensional spatial solitons in nonlocal nonlinear media, *Phys. Rev. E* **73** (2006) 066603.

31. N. F. Smyth, A. Piccardi, A. Alberucci and G. Assanto, Highly nonlocal optical response: Benefit or drawback? *J. Nonl. Opt. Phys. Mat.* **25** (2017) 1650043.

32. S. Chandrasekar, *An Introduction to the Study of Stellar Structure* (Dover Publications, Mineloa, New York, 2003).

33. V. F. Zaitsev and A. D. Polyanin, *Handbook of Exact Solutions for Ordinary Differential Equations* (Chapman Hall/CRC Press, 2002).

34. D. E. Panayotounakos, Exact analytic solutions of unsolvable classes of first and second order nonliPRE16near ODEs (Part I: Abels equations), *Appl. Math. Lett.* **18** (2005) 155–162.

35. D. E. Panayotounakos and T. I. Zarmpoutis, Construction of exact parametric or closed form solutions of some unsolvable classes of nonlinear ODEs (Abels nonlinear ODEs of the first kind and relative degenerate equations), *Int. J. Math. and Math. Sci.* **2011** (2011) 387429.

36. A. A. Minzoni, N. F. Smyth and A. L. Worthy, Modulation solutions for nematicon propagation in nonPRE16-local liquid crystals, *J. Opt. Soc. Amer. B* **24** (2007) 1549–1556.

37. C. J. Knickerbocker and A. C. Newell, Shelves and the Korteweg-de Vries equation, *J. Fluid Mech.* **98** (1980) 803–818.

38. R. Grimshaw, Internal solitary waves in a variable medium, *GAMM-Mitt.* **30** (2007) 96–109.

39. R. H. J. Grimshaw, *Solitary Waves in Fluids* (WIT Press, Boston, 2007).

40. F. Simoni, *Nonlinear Optical Properties of Liquid Crystals and Polymer Dispersed Liquid Crystals* (World Scientific Publishing, Singapore, 1997).

41. A. Alberucci, U. Laudyn, A. Piccardi, M. Kwasny, B. Klus, M. A. Karpierz and G. Assanto, Nonlinear continuous-wave optical propagation in nematic liquid crystals: Interplay between reorientational and thermal effects, *Phys. Rev. E* **96** (2017) 012703.

42. U. Laudyn, A. Piccardi, M. Kwasny, M. A. Karpierz and G. Assanto, Thermo-optic soliton routing in nematic liquid crystals, *Opt. Lett.* **43** (2018) 2296–2299.

43. U. Laudyn, A. Piccardi, M. Kwasny, B. Klus, M. A. Karpierz and G. Assanto, Interplay of thermo-optic and reorientational responses in nematicon generation, *MDPI Mater.* **11** (2018) 1837.

44. B. D. Skuse and N. F. Smyth, Two-colour vector soliton interactions in nematic liquid crystals in the local response regime, *Phys. Rev. A* **77** (2008) 013817.

45. G. Assanto, C. García-Reimbert, A. A. Minzoni, N. F. Smyth and A. L. Worthy, Lagrange solution for three wavelength solitary wave clusters in nematic liquid crystals, *Phys. D* **240** (2011) 1213–1219.

46. A. Alberucci, M. Peccianti, G. Assanto, A. Dyadyusha and M. Kaczmarek, Two-color vector solitons in nonlocal media, *Phys. Rev. Lett.* **97** (2006) 153903.

47. A. V. Mamaev, A. A. Zozulya, V. K. Mezentsev, D. Z. Anderson and M. Saffman, Bound dipole solitary solutions in anisotropic nonlocal self-focusing media, *Phys. Rev. A* **56** (1997) R1110–R1113.

48. A. Fratalocchi, A. Piccardi, M. Peccianti and G. Assanto, Nonlinearly controlled angular momentum of soliton clusters, *Opt. Lett.* **32** (2007) 1447–1449.

49. A. Fratalocchi, A. Piccardi, M. Peccianti and G. Assanto, Nonlinear management of the angular momentum of soliton clusters: Theory and experiments, *Phys. Rev. A* **75** (2007) 063835.

50. J. L. Synge and B. A. Griffith, *Principles of Mechanics* (McGraw-Hill, New York, 1949).

51. K. R. Simon, *Mechanics*, 2nd edn. (Addison Wesley, Reading, MA, 1960).

52. B. Fornberg and G. B. Whitham, Numerical and theoretical study of certain non-linear wave phenomena, *Phil. Trans. Roy. Soc. Lond. Ser. A* **289** (1978) 373–404.

53. T. F. Chan and T. Kerkhoven, Fourier methods with extended stability intervals for KdV, *SIAM J. Numer. Anal.* **22** (1985) 441–454.

54. N. F. Smyth and W. L. Kath, Radiative losses due to pulse interactions in birefringent nonlinear optical fibers, *Phys. Rev. E* **63** (2001) 036614.

55. T. Cazenave, *Semilinear Schrödinger Equations* (AMS, Providence, 2003).

56. G. Fibich, *The Nonlinear Schrödinger Equation. Singular Solutions and Optical Collapse* (Springer, New York, 2015).

57. C. Sulem and P. L. Sulem, *The Nonlinear Schrödinger Equation* (Springer, New York, 1999).

58. M. I. Weinstein, Nonlinear Shrödinger equations and sharp interpolation estimates, *Comm. Math. Phys.* **87** (1983) 567–576.

59. F. Bowman, *Introduction to Bessel Functions* (Dover, New York, 1958).

60. E. A. Kuznetsov, A. M. Rubenchik and V. E. Zakharov, Soliton stability in plasmas and hydrodynamics, *Phys. Rep.* **142** (1986) 103–165.

61. W. Krolikowski, O. Bang, N. I. Nikolov, D. Neshev, J. Wyller, J. J. Rasmussen and D. Edmundson, Modulational instability, solitons, and beam propagation in spatially nonlocal nonlinear media, *J. Opt. B: Quantum Semiclass. Opt. S* **6** (2004) 288–294.

62. A. I. Yakimenko, V. M. Lashkin and O. Prikhodko, Dynamics of two-dimensional coherent structures in nonlocal nonlinear media, *Phys. Rev. E* **73** (2006) 066605.

63. J. Ginibre and G. Velo, On a class of nonlinear Schrödinger equations with nonlocal interaction, *Math. Z.* **170** (1980) 109–136.

64. P. Panayotaros and T. R. Marchant, Solitary waves in nematic liquid crystals, *Physica D* **268** (2014) 106–117.

65. R. A. Adams and J. J. F. Fournier, *Sobolev Spaces* (Elsevier, Amsterdam, 2003).

66. S. K. Turitsyn, Spatial dispersion of nonlinearity and stability of multidimensional solitons, *Theor. Math. Phys.* **64** (1985) 226–232.

67. J. Ginibre and G. Velo, On a class of nonlinear Schrödinger equations I. The Cauchy problem, general case, *J. Funct. Anal.* **32** (1979) 1–32.

68. A. Stefanov and P. G. Kevrekidis, Asymptotic behavior of small solutions of the discrete nonlinear Schrödinger and Klein-Gordon equations, *Nonlinearity* **18** (2005) 1841–1857.

69. M. I. Weinstein, Excitation thresholds for nonlinear localized modes on lattices, *Nonlinearity* **12** (1999) 673–691.

70. P. G. Kevrekidis, M. I. Weinstein and Z. Rapti, Transient radiative behavior of Hamiltonian systems in finite domains, *Phys. Lett. A* **345** (2005) 1–9.

71. J. P. Borgna, P. Panayotaros, D. Rial and C. Sánchez de la Vega, Optical solitons in nematic liquid crystals: Model with saturation effects, *Nonlinearity* **31** (2018) 1535.

72. A. Alberucci, A. Piccardi, N. Kravets, O. Buchnev and G. Assanto, Soliton enhancement of spontaneous symmetry breaking, *Optica* **2** (2015) 783–789.

73. N. Kravets, A. Piccardi, A. Alberucci, A. Buchnev, M. Kaczmarek and G. Assanto, Bistability with optical beams propagating in a reorientational medium, *Phys. Rev. Lett.* **113** (2014) 023901.

74. P. S. Jung, W. Krolikowski, U. A. Laudyn, M. Trippenbach and M. A. Karpierz, Supermode spatial optical solitons in liquid crystals with competing nonlinearities, *Phys. Rev. A* **95** (2017) 023820.

75. I. B. Burgess, M. Peccianti, G. Assanto and R. Morandotti, Accessible light bullets via synergetic nonlinearities, *Phys. Rev. Lett.* **102** (2009) 203903.

76. M. Peccianti, I. B. Burgess, G. Assanto and R. Morandotti, Space-time bullet trains via modulation instability and nonlocal solitons, *Opt. Express* **18** (2010) 5934–5941.

77. M. Peccianti, A. Pasquazi, G. Assanto and R. Morandotti, Enhancement of third harmonic generation in nonlocal spatial solitons, *Opt. Lett.* **35** (2010) 3342–3344.

78. S. Slussarenko, A. Alberucci, C.-P. Jisha, P. Piccirillo, E. Santamato, G. Assanto and L. Marrucci, Guiding light via geometric phases, *Nat. Photon.* **10** (2016) 571–575.

79. A. Alberucci, C. P. Jisha, L. Marrucci and G. Assanto, Electromagnetic confinement via spin-orbit interaction in anisotropic dielectrics, *ACS Photon.* **3** (2016) 2249–2254.

80. S. Bolis, T. Virgili, S. Rajendran, J. Beeckman and P. Kockaert, Nematicon-driven injection of amplified spontaneous emission into an optical fiber, *Opt. Lett.* **41** (2016) 2245–2248.

81. S. Perumbilavil, A. Piccardi, R. Barboza, O. Buchnev, G. Strangi, M. Kauranen and G. Assanto, Beaming random lasers with soliton control, *Nature Comms.* **9** (2018) 3863 (1–7).

82. S. Perumbilavil, A. Piccardi, O. Buchnev, G. Strangi, M. Kauranen and G. Assanto, Spatial solitons to mold random lasers in nematic liquid crystals, *Opt. Mat. Express* **8** (2018) 3864–3878.

G. Assanto, P. Panayotaros & N. F. Smyth